Ref.TH.1278-CERN

PROPERTIES OF DUAL MULTILOOP AMPLITUDES

V. Alessandrini *)

CERN - Geneva
and
University of Geneva

and

D. Amati

CERN - Geneva

A B S T R A C T

Previous results on the dual multiloop amplitude are extended by obtaining, from the unitarization procedure, the measure and domain of integration. The singularities of the amplitude, which arise from end points in the integration domain, are discussed by exploiting the simple geometrical interpretation of the theory. In particular, we investigate the singularities which give rise to divergences in planar diagrams as well as Pomeranchuk-like singularities in non-planar ones.

---

*) On leave of absence from University of La Plata, Argentina. Partially supported by the Swiss National Fund.

Ref.TH.1278-CERN
25 January 1971

1. INTRODUCTION

In spite of the apparent complexity of the M loop generalized Veneziano formula [1)-3)], it has recently been shown [1),2)] that the most important part of the integrand - the one that depends on the momenta of external particles - has a simple geometrical interpretation. Indeed, the quantity raised to the power $p_i \cdot p_j$ in the multiloop integrand turns out to be simply the exponential of certain harmonic functions defined on a closed Riemann surface topologically equivalent to a sphere with M handles. These harmonic functions are the so-called third Abelian integrals, which are simply the solution of the classical flow problem on the surface with a source and a sink of equal but opposite strengths. These harmonic functions are simply related to the Newmann function of each of the two copies of a surface with boundaries obtained, loosely speaking, by cutting the closed surface into two symmetrical halves. In this way, the equivalence of the operator formalism with the original Nielsen analogue model [4)] was established.

In Refs. 1) and 2) this result was established for the multiloop integrand but only part of the measure of integration was considered. A general discussion was given of the divergence factors - generalized partition functions - that depend only on the multipliers of the group of automorphisms, but the part of the integration measure that depends on Koba-Nielsen variables of external particles was not explicitly considered. The first purpose of this paper is to discuss with more detail the measure of integration and the duality properties of multiloop amplitudes and to give a general prescription on how should the most general multiloop amplitude be integrated.

The measure and domain of integration of multiloop amplitudes are discussed in Section 2. The domain of integration can be understood as follows: the M loop amplitude has an associated Riemann surface given by a sphere with M handles. The Koba-Nielsen variables z_i of external particles can be identified with points on the surface. If the surface is kept fixed the z_i's run along

certain closed paths - or cycles - on the surface that split it into two symmetrical halves and that correspond to the boundaries of the original open surface of the analogue model. The z_i's are integrated along these cycles on the surface in such a way that the cyclic order of the z_i's that are on the same cycle is maintained, and that each configuration is counted only once. Different sets of cycles - there are several ways of splitting a sphere with M handles into two symmetrical halves - and different partitions of Koba-Nielsen variables on the cycles correspond to different M loop amplitudes. Finally, the surface is also varied by integrating over a remaining set of $(3M-3)$ variables - the so-called Riemann moduli - that describe conformally inequivalent configurations of the Riemann surface.

The second purpose of this paper is to start a general discussion on singularities and divergencies of multiloop amplitudes, and this problem is discussed in Section 3. The integration over the Koba-Nielsen variables of external particles gives rise only to poles, and the new singularities, specific of multiloop amplitudes - like normal threshold cuts - arise from the integration over the surface parameters. Indeed, all these unitarity singularities can be associated with an end point in the domain of the Riemann moduli that corresponds to the vanishing of one or more handles. A short discussion is given in Section 3 of the different mechanisms that generate these unitarity singularities.

The bulk of Section 3 is devoted to the analysis of a new class of singularities that are characteristic of dual theories and that are not unitarity singularities in the sense that they are not associated with the intermediate states of the Born approximation. These singularities are the so-called Pomeranchuk-like singularity in non-planar diagrams or the exponential divergences of the integrand in the planar ones, and they are discussed in detail for the case of the N loop diagram with $(N+1)$ boundary cycles on the associated Riemann surface, using the results of domain variational theory.

This branch of mathematics [5] gives the behaviour of invariant functions on a Riemann surface when the surface is varied, and is, therefore, particularly suited to the analysis of all singularities coming from end points of integration in the Riemann moduli.

Domain variational theory can be applied at once to obtain the behaviour of the momentum-dependent part of the multiloop integrand near the end points of integration, because this part of the integrand is given in terms of invariant functions on the Riemann surface. However, the measure of integration is not an invariant differential and its behaviour near the end points of integration is simply obtained only in a few special cases. This problem is particularly evident for the case of the non-unitary singularities we are interested in; and the way in which we have solved it, is also explained at length in Section 3. Our methods allow us to carry out a full investigation of Pomeranchuk-like singularities and divergences for the set of multiloop amplitudes we are considering. Using domain variational theory, we find the most singular part of the integrand in the cases in which the integral diverges, and we are, therefore, able to write counterterms that render the integrals finite in different limits of integration, and that also have a very simple interpretation in terms of invariant functions on a Riemann surface.

All the ingredients of the theory of functions on Riemann surfaces and of automorphic functions that are useful in multiloop theory have been presented in Ref. 2) - hereafter referred to as I - and we shall use here all the conventions and notations used in that paper. We have also included two Appendices. Appendix A contains a slightly refined version of the multiloop calculations carried out in Refs. 1) and 2) and is included mainly for the sake of completeness. Appendix B contains the discussion of some technical points associated with the renormalization problem.

2. INTEGRATION DOMAIN OF MULTILOOP AMPLITUDES

The purpose of this section is to consider the measure and the domain of integration of multiloop amplitudes. We shall use here the notations and conventions of I.

a. The General Multiloop Amplitude

The most general M loop amplitude in the dual resonance model can be calculated by sewing M pairs of Reggeons in an N Reggeon vertex, leaving $N' = N-2M$ external Reggeons which can eventually be restricted to be in the ground state corresponding to the basic scalar particle of the theory.

Several different expressions for the N Reggeon vertex have been considered recently [6),7),8)] in the literature, which turn out to be equivalent in the calculation of scalar tree diagrams. Indeed, they all differ from one another ba gauge operators associated with external Reggeon legs, which, of course, are irrelevant when the Reggeons are coupled to physical states made out of scalar particles. However, previous experience with one-loop diagrams shows that gauge operators that are trapped inside a closed loop give rise to a modification of the integration measure. This is the way in which factors representing the absence of spurious states show up in the measure whenever a non-planar loop is computed using the Hermitian twisted propagator [9)] $P(x) = x^{H}\theta(1-x)^{W}$. It is, therefore, clear that a definite criterion must be used in the choice of the N Reggeon vertex.

The criterion we are looking for is given by the two following fundamental requirements, both implied in the KSV unitarization program [10)] for the dual resonance model:

a) the multiloop amplitude must be independent of the particular set of Reggeons that one chooses to sew;

b) the multiloop amplitudes should exhibit duality properties in all internal lines.

These requirements are automatically fulfilled if the N Reggeon vertex satisfies

a') complete factorization (i.e., of the operator part as well as the measure);

b') operatorial duality.

Property a') guarantees a) for the multiloop amplitude. Indeed, by multiple factorization the N Reggeon vertex operator can be turned down into a series of N-2 three Reggeon vertices V joined by N-3 propagators P. Then, the sewing implies to close the loops with other propagators *) and the result, being completely symmetric in all lines, shows that it is irrelevant to identify one or the other propagator as the one originated by the sewing.

For operational duality we mean that, for amplitudes constructed with three-Reggeon vertices and propagators, the relation

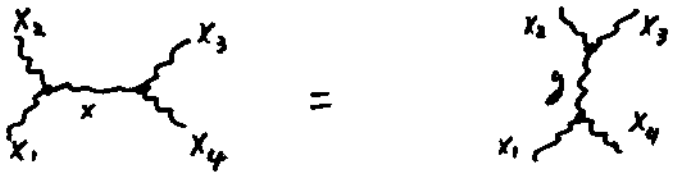

is satisfied identically in the operators $a_1,\ldots,a_4$ and in the Chan variables $x_1,\ldots,x_4$ of the external lines before any integration is carried out, provided x and y are related by the KSV change of variables [10]. This property remains true after further sewings of the external Reggeons, and guarantees the invariance of the tree or multiloop amplitudes when an arbitrary internal line is dualized. The symmetric N Reggeon vertex that satisfies properties a') and b') is the one proposed by Olive [8] which we shall use from now on with a slightly different notation. Other versions of the N Reggeon vertex [6),7)] satisfy also properties a') and b') but only up to gauge operators attached to the external Reggeon lines, and the duality properties of the whole multiloop amplitude are therefore not automatically guaranteed. Since, as we said before, they differ from Olive's vertex by some gauge

---

*) We defer to Ref. 9) the discussion on twist and gauge properties, of vertices and propagators as well as factorization of tree amplitudes and definition of sewing.

operators associated to external lines, there will be some modifications in the integration measure of the multiloop amplitude. We shall discuss in detail this modification for the planar multiloop amplitude in Section d. of this Chapter.

In Olive's formulation [8], each Reggeon is characterized by means of two adjacent Koba-Nielsen variables z_i, β_i running over the unit circle, and which can be thought of as the Koba-Nielsen variables of the two scalars (or quarks?) out of which the Reggeon has been factorized. Keeping track of these two Koba-Nielsen variables allows one to define the Chan variable of the Reggeon as

$$x_i = (\beta_i, z_i, \beta_{i-1}, z_{i+1}) \tag{2.1}$$

where, as usual, we use the notation

$$(a,b,c,d) = \frac{(a-b)(c-d)}{(a-c)(b-d)} \tag{2.2}$$

If the i^{th} Reggeon is in its ground state, its Chan variable $x_i = 0$ and, consequently, we have $z_i = \beta_i$, that is to say, we recover a single Koba-Nielsen variable for the scalar particle. Since we shall ultimately put all non-sewn Reggeons in their ground state, this extra variable will be of relevance only for sewn Reggeons and will be related to their Chan variables. One of the two variables, say z_i, can be thought of as the point where the Reggeon is implanted. Moreover, Reggeons should be twisted in Olive's vertex using the Hermitian twisting operator [9] $\Theta(x_i) = \Omega_i (1-x_i)^W$ and this interchanges the role of the z_i and β_i variables.

We then write the N Reggeon vertex as

$$V_N = \int \frac{dz_1 \ldots [dz_a] \ldots [dz_b] \ldots [dz_c] \ldots dz_N}{\prod_{i=1}^{N} (z_{i+1} - z_i) \quad (1-Q)} (z_a - z_b)(z_b - z_c)(z_c - z_a) \cdot$$

$$\cdot \left[- \prod_{i=1}^{N} \frac{z_{i+1} - \beta_{i-1}}{z_i - \beta_{i-1}} \right]^{\alpha} \cdot \exp \frac{1}{2} \sum_{\substack{(i,j)=1 \\ (i \neq j)}}^{N} a^{(i)+} U^i V^j a^{(j)+} |0_{1 \ldots N}\rangle \tag{2.3}$$

In (2.3), z_a, z_b, z_c represent the Koba-Nielsen variables of three arbitrary Reggeons which are not integrated.

The variables in Eq. (2.3) satisfy the following cyclic order over the unit circle

$$z_1, \beta_1, z_2, \beta_2 \ \ldots \ z_i, \beta_i, \ \ldots \ z_N, \beta_N \tag{2.4}$$

and the integration region over z_i covers the whole unit circle subject to the condition (2.4).

The quantity Q in (2.3) is defined by

$$Q = \prod_{i=1}^{N} \frac{z_i - \beta_i}{z_{i+1} - \beta_{i-1}} \tag{2.5}$$

and, therefore, it is equal to zero if at least one the Reggeon in the vertex is in its ground state, because, as said before, in this case its z and β variables coincide. Due to the fact that we shall put all unseen Reggeons in their ground states, we can forget from now on the Q factor in (2.3).

The operators $a^{(i)+}$ in (2.3) belonging to every Reggeon i are really a set of operators [9] $a^{(i)+}_{n,\mu}$ where $n = 0,1,2\ldots$ and $\mu = 0,1,2,3$ (μ is a Lorentz index). The zero mode is coupled to the momentum of the Reggeon, i.e., a Reggeon with momentum p is an eigenstate of $a_{0,\mu}$ with eigenvalue p_μ. $U^{(i)}$ and $V^{(i)}$ are infinite matrices whose matrix elements are defined in terms of 2×2 matrices generating projective transformations [9]. Each infinite matrix C has an associated 2×2 matrix

$$\tau = \begin{pmatrix} a & b \\ c & d \end{pmatrix} \tag{2.6}$$

in terms of which its matrix elements are defined as

$$\frac{1}{\sqrt{n}} \left(\frac{az+b}{cz+d} \right)^n = C_{n0} + \sum_{m=1}^{\infty} C_{nm} \frac{z^m}{\sqrt{m}} \quad , \quad n \geq 1 \tag{2.7}$$

$$C_{on} = (C^T)_{no} = \frac{1}{\sqrt{n}}\left(-\frac{c}{d}\right)^n$$

$$C_{oo} = \log\left|\frac{d}{\sqrt{ad-bc}}\right| \tag{2.8}$$

The U^i and V^j matrices can be written as

$$U^i = \begin{pmatrix} \xi_i & -\xi_i\beta_{i-1} \\ 1 & -z_i \end{pmatrix} \equiv \begin{bmatrix} \beta_{i-1} & z_i & z_{i+1} \\ 0 & \infty & 1 \end{bmatrix}$$

$$V^j = \begin{pmatrix} \xi_j\beta_{j-1} & -z_j \\ \xi_j & 1 \end{pmatrix} \equiv \begin{bmatrix} \infty & 0 & 1 \\ \beta_{j-1} & z_j & z_{j+1} \end{bmatrix} \tag{2.9}$$

where $\xi_i = (z_i - z_{i+1})/(\beta_{i-1} - z_{i+1})$.

In computing matrix elements of products of matrices the correct procedure is first to multiply the corresponding 2×2 matrices and then to apply Eqs. (2.7)-(2.9).

The multiloop amplitude can now be calculated by sewing pairs of Reggeons as done in Refs. 1) and 2). A slightly refined version of the calculation is given in Appendix A. After sewing M pairs of Reggeons with Koba-Nielsen variables z_μ, β_μ and $\tilde{z}_\mu$, $\tilde{\beta}_\mu$ by connecting them with a (twisted or untwisted) propagator [9] with associated Chan variable x_μ, and after the loop momentum integration is done, one obtains the result

$$A_{M,N'} = \int_0 \prod'_{\mu\in[M]} \frac{dx_\mu}{x_\mu^{1+a}(1-x_\mu)^{1-a}} \int \frac{\prod_{i=1}^{N} dz_i / dV_{abc}}{\prod_{i=1}^{N}(z_{i+1}-z_i)}$$

$$\cdot \left[-\prod_{i=1}^{N} \frac{z_{i+1}-\beta_{i-1}}{z_i-\beta_{i-1}} \right]^a \prod_{i\in[N']} \exp \frac{\mu^2}{2} \varphi_i \cdot \frac{\exp -\frac{1}{2}\sum_{i,j\in N'} p_i\cdot p_j\, V(z_i,z_j;z_o,z_o')}{(\det A)^2 \prod'_{\alpha} \prod'_{q=1} (1-K_\alpha^n)} \tag{2.10}$$

where $[M]$ and $[N']$ indicate the set of indices corresponding to the sewn and unsewn Reggeons. Moreover, $\varphi_i = (U^i)_{oo} + (V^i)_{oo}$, and $V(z_i,z_j;z_o,z_o')$ is the Green function of a sphere with M handles if the indices i, j are different and the regular part of V if the indices i, j are equal. We remind the reader that the Green function of a closed Riemann surface is defined in terms of its Abelian integrals [5] as

$$V(z_i;z_j,z_o,z_o') = \mathrm{Re}\,\Omega_{z_j z_o}(z_i) - \mathrm{Re}\,\Omega_{z_j z_o'}(z_o) \tag{2.11}$$

and the regular part is defined as $V-\log|1-(z_i/z_j)|$. The possibility of fixing three arbitrary variables z_a, z_b, z_c is the origin of the volume element

$$dV_{abc} \equiv \frac{dz_a\, dz_b\, dz_c}{(z_a-z_b)(z_b-z_c)(z_c-z_a)}$$

in Eq. (2.10).

We have taken z_o, z_o' to be two arbitrary points on the surface, that is to say, two ordinary points in the complex plane of its group of automorphisms (this will be clear in what follows). The independence of z_o, z_o' is guaranteed in this case by momentum conservation. For the case of the sphere with no handles, $\exp V(z_i,z_j;z_o,z_o')$ is just the anharmonic ratio of the four points indicated in the argument of the Green function.

We have written our result in terms of the Green function of a closed Riemann surface - the "double" of the open Riemann surface

of the analogue model [2),5)] - because they may be more meaningful than the original surfaces of the analogue model. Indeed, we shall see that $\exp V$ has to be integrated along well-defined paths on the closed Riemann surface.

b. The Group of Automorphisms

The explicit form of the Green function V was given in I in terms of the group of automorphism which defines the Riemann surface. This group is the infinite set of projective transformations T_α defined by arbitrary products of the M generators T_μ and their inverses T_μ^{-1}. Every generator originates from a pair of sewn Reggeons and is given by

$$T_\mu = \begin{bmatrix} \infty & 0 & 1 \\ \hat{\beta}_{\mu-1} & \hat{z}_\mu & \hat{z}_{\mu+1} \end{bmatrix} \begin{bmatrix} \beta_{\mu-1} & z_\mu & z_{\mu+1} \\ x_\mu & 1 & 0 \end{bmatrix} \tag{2.12a}$$

if the pair of Reggeons with Koba-Nielsen variables z_μ, β_μ and $\tilde{z}_\mu$, $\hat{\beta}_\mu$ are sewn with the propagator [9)]

$$P = \int_0^1 dx_\mu \, x_\mu^{L_0} \, \Theta(x_\mu) \tag{2.13a}$$

and by

$$T_\mu = \begin{bmatrix} \infty & 0 & 1 \\ \tilde{\beta}_{\mu-1} & \hat{z}_\mu & \tilde{z}_{\mu+1} \end{bmatrix} \begin{bmatrix} \beta_{\mu-1} & z_\mu & z_{\mu+1} \\ 0 & \infty & x_\mu \end{bmatrix} \tag{2.12b}$$

if the Reggeons are sewn with the propagator [9)]

$$D = \int_0^1 dx_\mu \, x_\mu^{L_0} \tag{2.13b}$$

We remind here the reader that, due to the symmetric structure of the vertex [8)], the first case (2.12a) corresponds to an untwisted line and the second (2.12b) to a twisted one.

Let us analyze the transformation T_μ. The Chan variable x_μ of each Reggeon is related to the two Koba-Nielsen variables z_μ, β_μ and the neighbouring variables $\beta_{\mu-1}$ and $z_{\mu+1}$ by (2.1). When two Reggeons are sewn, one must impose the condition that their Chan variables coincide, and this means that the parameters β_μ and $\hat{\beta}_\mu$ are related to the integration variable x_μ in (2.10) by

$$x_\mu = (\beta_\mu, z_\mu, \beta_{\mu-1}, z_{\mu+1}) = (\hat{\beta}_\mu, \hat{z}_\mu, \hat{\beta}_{\mu-1}, \hat{z}_{\mu+1}) \tag{2.14}$$

Condition (2.4) implies

$$0 \leq x_\mu \leq 1 \tag{2.15}$$

By using (2.14) we can rewrite (2.12a) and (2.12b) as

$$T_\mu = \begin{bmatrix} \beta_\mu & z_\mu & z_{\mu+1} & \beta_{\mu-1} \\ \hat{\beta}_{\mu-1} & \hat{z}_{\mu+1} & \hat{z}_\mu & \hat{\beta}_\mu \end{bmatrix} \tag{2.16a}$$

for an untwisted sewn Reggeon and

$$T_\mu = \begin{bmatrix} \beta_\mu & z_\mu & \beta_{\mu-1} & z_{\mu+1} \\ \hat{z}_{\mu+1} & \hat{\beta}_{\mu-1} & \hat{z}_\mu & \hat{\beta}_\mu \end{bmatrix} \tag{2.16b}$$

for a twisted one.

In Eqs. (2.16a) and (2.16b) any one of the columns is implied by the other three and the equality given by Eq. (2.14). It is also convenient to eliminate x_μ in the measure of integration in favour of β_μ or $\tilde{\beta}_\mu$, using the relation

$$\frac{dx_\mu}{x_\mu(1-x_\mu)} = \frac{(z_{\mu+1}-z_\mu)\,d\beta_\mu}{(z_\mu-\beta_\mu)(\beta_\mu-z_{\mu+1})} = \frac{(\tilde{z}_{\mu+1}-\tilde{z}_\mu)\,d\tilde{\beta}_\mu}{(\tilde{z}_\mu-\tilde{\beta}_\mu)(\tilde{\beta}_\mu-\tilde{z}_{\mu+1})} \tag{2.17}$$

In Figures 1a and 1b we have shown the relative order of the different variables on the unit circle and the correspondences implied by Eqs. (2.16a) and (2.16b), respectively. The arrows indicate how the points are mapped into each other by the application of T_μ.

Every generator T_μ depends on three parameters. Instead of z_μ, $\tilde{z}_\mu$ and x_μ, originated by the sewing procedure, we could introduce the two invariant points ξ_μ, η_μ and the multiplier K_μ. They are defined by [11]

$$\frac{T_\mu(z)-\xi_\mu}{T_\mu(z)-\eta_\mu} = K_\mu\,\frac{z-\xi_\mu}{z-\eta_\mu} \tag{2.18}$$

with the convention

$$|K_\mu| \leq 1 \tag{2.19}$$

By examining in Figs. 1a and 1b how points transform under T_μ, it is easy to locate the position of the invariant points ξ_μ, η_μ on the unit circle relative to the other variables that we are considering. We can see that, in general, they are located

between z_μ and β_μ and between $\tilde{z}_\mu$ and $\tilde{\beta}_\mu$. It follows from (2.4) that the invariant points ξ_μ, η_μ are ordered, with respect to the Koba-Nielsen variables of all the remaining Reggeons not sewn by the generator T_μ, in exactly the same way as the Koba-Nielsen variables z_μ and $\tilde{z}_\mu$ of the sewn Reggeons. All our generators T_μ leave the unit circle invariant and this is therefore a property of all members T_α of the group. This is the reason why every transformation depends on only three real parameters (phases of ξ_μ and η_μ and the real multiplier K_μ), K_μ being positive for (2.16a) and negative for (2.16b).

There are several advantages in using the invariant points ξ_μ, η_μ and the multiplier K_μ as integration variables instead of the old Koba-Nielsen variables z_μ, $\tilde{z}_\mu$ and the Chan variable x_μ as in (2.10). With this later set of variables the situation is rather aesthetically unpleasant because it is not quite clear what role should the Chan variables x_μ play under over-all projective transformations. With invariant points and multipliers the situation is more transparent; an over-all projective transformation carried out in the complex z plane where the group of automorphisms is defined is equivalent to a similarity transformation of the elements of the group [11]. Since the multiplier is a function of the trace and the determinant of the 2×2 matrices that defines the group element, it is left invariant under such a similarity transformation [11]. Due to the over-all projective invariance of the integrand, we can arbitrarily fix three points which - except for the case $M=1$ - can be chosen to be three invariant points. For $M=1$ we have only two invariant points and we are therefore forced to fix in addition the Koba-Nielsen variable z_i of some external particle.

As explained at length in I, automorphic functions with respect to these groups with M generators define single-valued functions on a Riemann surface topologically equivalent to a sphere with M handles. The Koba-Nielsen complex plane is simply the complex plane in which these groups of automorphisms are defined.

More than that, the generators T_μ of the group of automorphism provide us with a concrete parametrization of the surface. It can be shown that two Riemann surfaces are conformally equivalent if and only if their corresponding groups of automorphisms are connected by a similarity transformation [11]. We have seen before that this corresponds to an over-all projective transformation of the multiloop integrand. Therefore, when three invariant points are kept fixed because of the over-all projective invariance of the integrand, the remaining $(3M-3)$ fixed points and multipliers parametrize conformally inequivalent Riemann surfaces. Projective invariance of the multiloop integrand, therefore, means that one is integrating over conformally inequivalent configurations of the surface. In the one-loop case the surface depends on only one parameter which describes its conformally inequivalent configurations. In general, the $(3M-3)$ parameters are complex; but, in our case, they are real and this means that we are dealing with symmetrical Riemann surfaces, that is to say, surfaces that can be thought of as the double of some open surfaces with boundaries.

At this stage the main advantage of using invariant points and multipliers as independent variables should also be clear: the variables describing configurations of the surface are decoupled from the remaining variables, the Koba-Nielsen variables z_i of external particles, that correspond to points on the surface. For every set of $(3M-3)$ surface parameters we shall find a region of integration for the external variables z_i that is dictated by the sewing procedure and the extra requirement that every configuration of the points on the surface is counted only once. Then we shall discuss the integration over the remaining $(3M-3)$ surface parameters.

Finally, we want to emphasize here a point discussed at length in I concerning the connection between Burnside's group of automorphisms [12] and the Riemann surface. Consider the sphere with M handles represented in Fig. 2, where we have drawn a set of canonical cycles $C_{2\mu-1}$, $C_{2\mu}$ $(\mu = 1,\ldots,M)$. The whole Riemann surface corresponds to the fundamental region of the group, which is

the exterior of all the isometric circles of T_μ and T_μ^{-1} ($\mu = 1,\ldots,M$) if they are all non-intersecting. This is not, however, an essential requirement because the fundamental region can also be defined if isometric circles corresponding to different generators intersect [11]. Any other region obtained by mapping the fundamental region by an element of the group, $T_\alpha(z)$, is as good as the first one to represent the surface. Indeed, z and $T_\alpha(z)$ correspond to the same point on the Riemann surface. The infinitely many regions so obtained fill the complex plane except for some points that are the limit points of the group. The isometric circles of T_μ and T_μ^{-1}, to be denoted by I_μ and I_μ^{-1}, become on the surface the "vertical" canonical cycles $C_{2\mu-1}$. Paths joining on the complex plane homologous points of I_μ and I_μ^{-1} become, on the surface, the "horizontal" canonical cycles $C_{2\mu}$.

The group of automorphisms that we find corresponds to a cutting of the surface along the vertical $C_{2\mu-1}$ canonical cycles, whereas the open surface of the analogue model (in the planar case, for example) is obtained by cutting the surface "horizontally" along the $C_{2\mu}$ cycles and a closed cycle that goes around all handles. These cycles become the boundaries of the open surface, and this is why we shall refer to them sometimes as "boundary lines" though, of course, our surface has no boundaries. In particular, we can see that arcs of the unit circle joining I_μ and I_μ^{-1} over which external variables z_i run, will become boundary lines in our language, and will correspond to boundaries of the open surface of the analogue model.

c. The Region of Integration

i) The one-loop orientable diagrams

Let us first consider the example of the one-loop orientable diagrams, whose group of automorphisms is exhibited in Fig. 3. If we denote by ξ, η, K the invariant points and multipliers we can draw the two isometric circles I and I^{-1} (with the same

radii) which are perpendicular to the unit circle. The intersecting points are homologous to each other in the sense that

$$A' = T(A) \qquad B' = T(B)$$

where T is the transformation defined by (2.18) in terms of ξ, η and K (K positive in this case).

Let us now fix $z_{\mu+1}$ arbitrarily in the BB' segment. Then $\tilde{z}_\mu$ of Fig. 1a is

$$\tilde{z}_\mu = T(z_{\mu+1})$$

The condition that we had before sewing, that is to say, that all z_i, starting from $z_{\mu+2}$ up to $\tilde{\beta}_{\mu-1}$, are integrated in all possible positions of the unit circle provided their relative order is preserved and they do not overcome $\tilde{z}_\mu$, is reflected in the fact that they are integrated between $z_{\mu+1}$ and $T(z_{\mu+1})$ keeping their relative order.

On the Riemann surface this is equivalent to saying that, fixing $z_{\mu+1}$, all the variables from $z_{\mu+1}$ up to $\tilde{\beta}_{\mu-1}$ range over a closed cycle.

Similarly, fixing $\tilde{z}_{\mu+1}$, all variables from $\tilde{z}_{\mu+1}$ up to $\beta_{\mu-1}$, range over another closed cycle. Now we must integrate over $z_{\mu+1}$ and $\tilde{z}_{\mu+1}$. One of them can be kept fixed because of over-all projective invariance but the other, say $z_{\mu+1}$, can, in principle, go from η to ξ. This would imply, on the surface, that it would go around its corresponding cycle an infinite number of times due to the fact that invariant points are also limit points, that is to say, accumulation points of fundamental regions [11]. This reflects the infinite multiple counting first encountered by Kaku and Thorn [13]. In order to avoid it we must impose the restriction that $z_{\mu+1}$ also goes only once over the boundary cycle. This implies in Fig. 2 that $z_{\mu+1}$ also goes - as the other variables do - over a segment of the unit circle in the fundamental region, i.e., limited by a point and its transform as, for instance, the segment BB'.

As discussed in I we can visualize the surface as a torus (see Fig. 4). The two boundaries are shown in dotted lines and are such that if we cut the surface around both of them we are left with two separated symmetric open surfaces. The prescription we obtained can be interpreted by saying that the dual amplitude we are discussing is obtained by allowing the external variables which are on a boundary to be integrated only once over all possible positions on that boundary cycle keeping their relative order fixed.

A different cyclic ordering of external variables in a boundary corresponds to a different dual amplitude. Furthermore, a different partition of external variables between the two boundaries correspond to a different family of dual amplitudes. The planar loop amplitude, for instance, is obtained when all variables are on only one boundary cycle. This is the particular case when the two sewn Reggeons (of Fig. 1a) are contiguous. In this case $\tilde{z}_\mu = z_{\mu+1}$, $\tilde{\beta}_\mu = \beta_{\mu+1}$ so that I_μ given by (2.16a) becomes

$$I_\mu = \begin{bmatrix} \beta_\mu & z_\mu & z_{\mu+1} & \beta_{\mu-1} \\ \beta_\mu & z_{\mu+2} & z_{\mu+1} & \beta_{\mu+1} \end{bmatrix} \tag{2.20}$$

From (2.20) it is obvious that

$$\eta_\mu = \beta_\mu \quad , \quad \xi_\mu = z_{\mu+1} \tag{2.21}$$

Moreover, from (2.20) $z_{\mu+2} = T(z_\mu)$ and $\beta_{\mu+1} = T_\mu(\beta_{\mu-1})$ so that, using (2.18) and (2.21) we find

$$K_\mu = (z_\mu, \beta_\mu, z_{\mu+1}, z_{\mu+2}) = (\beta_{\mu-1}, \beta_\mu, z_{\mu+1}, \beta_{\mu+1}) \tag{2.22}$$

In this case, the Jacobian of the transformation from the volume element $dz_\mu\, d\tilde{z}_\mu\, dx_\mu$ that originally occurred in the loop calculation to $d\xi_\mu d\eta_\mu dK_\mu$ is particularly simple. Indeed, by using Eqs. (2.17), (2.21) and (2.22) we find

$$\frac{dx_\mu\, dz_\mu\, d\tilde{z}_\mu}{x_\mu(1-x_\mu)} = \frac{dK_\mu\, d\xi_\mu d\eta_\mu}{K_\mu(1-K_\mu)} \frac{(z_\mu-\xi_\mu)(z_\mu-z_{\mu+2})}{(\eta_\mu-\xi_\mu)(z_{\mu+2}-\eta_\mu)} \tag{2.23}$$

where, in the right-hand side, z_μ must be understood as $z_\mu = T_\mu^{-1}(z_{\mu+2})$ where T_μ is determined by ξ_μ, η_μ and K_μ.

ii) Non-orientable one-loop example

Let us now discuss briefly the one-loop non-orientable case. Given ξ, η and K (now $K<0$) we can again represent the isometric circles as in Fig. 3, but now the intersecting points are related by

$$A' = T(B) \quad , \quad B' = T(A)$$

It is clear from this identification that, on the surface, all external variables will run over only one boundary cycle. Indeed, as seen in Fig. 1b, the point $\beta_{\mu-1}$ is the same as the point $\tilde{z}_\mu = T(\beta_{\mu-1})$ and, therefore, all external variables on the upper side of the figure can be transported to the lower side by the action of T. The last one, $T(\tilde{z}_{\mu+1})$ will be bounded to come before $T(\tilde{\alpha}_\mu) = T^2(z_{\mu+1})$. We notice that $T^2_{\xi\eta K} = T^2_{\xi\eta|K|}$ and, also, that the point $T_{\xi\eta|K|}(z_{\mu+1})$ would be in the southern hemisphere of Fig. 1b, somewhere in between $z_{\mu+1}$ and $T^2_{\xi\eta|K|}(z_{\mu+1})$. Then, fixing $z_{\mu+1}$, we can say that the integration region of all the other external particles is the boundary line on the surface which starts at the point $z_{\mu+1}$,

goes through $T_{\xi\eta|K|}(z_{\mu+1})$ and closes back at $T^2_{\xi\eta K}(z_{\mu+1})$.

We illustrate in Fig. 5 the boundary cycle on the torus: it cuts two Möbius strips from it.

The points $T_{\xi\eta|K|}(z_i)$ [as the $T_{\xi\eta|K|}(z_{\mu+1})$ discussed before] subdivide the integration region in subregions that show different dual singularities. For the three-point one-loop non-orientable diagram, for instance, the singularities of the different twisted configurations of the triangle diagram [14] - all dual to each other - can be associated with the subdivision of the integration region as follows:

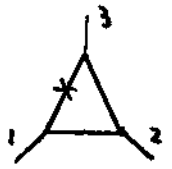

$$\Rightarrow \quad z_1 < z_2 < z_3 < T_{\xi\eta|K|}(z_1)$$

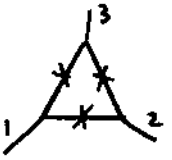

$$\Rightarrow \quad z_1 < z_2 < T_{\xi\eta|K|}(z_1) < z_3 < T_{\xi\eta|K|}(z_2)$$

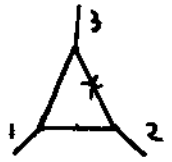

$$\Rightarrow \quad z_1 < z_2 < T_{\xi\eta|K|}(z_1) < T_{\xi\eta|K|}(z_2) < z_3 < T^2_{\xi\eta K}(z_1)$$

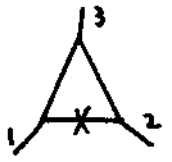

$$\Rightarrow \quad T_{\xi\eta|K|}(z_1) < z_2 < z_3 < T^2_{\xi\eta|K|}(z_1)$$

We do not find multiple counting in the non-orientable one-loop, due to the freedom to fix an external particle ($z_{\mu+1}$ in the preceding discussion). But, if some extra sewings were performed this would replace some other z_i by invariant points of other transformations which would be kept fixed by fixing the surface.

Then, $z_{\mu+1}$ could approach ξ_μ and η_μ covering, therefore, an infinite number of times the boundary we discussed. Again, we would add the extra condition that the integration region counts every configuration only once so that $z_{\mu+1}$ goes also only once through the boundary line.

We have discussed, up to now, the integration region of external variables, which are some boundary cycles on the surface. The integration over the surface parameters is straightforward in the single loop case due to the fact that there is only one parameter K which may vary between 0 to 1 for the orientable case and 0 and -1 for the non-orientable one. This limitation is obvious, due to the fact that by definition the multipliers of the transformations (2.16a), (2.16b) are always defined to be in modulus less than one. Including regions with $|K| > 1$ would imply multiple counting of conformally inequivalent configurations of the surface. Moreover, the partition function that occurs in the measure has a natural boundary on the circle $|K| = 1$ so that the integration cannot possibly be extended beyond it.

iii) General prescription for the integration region

The discussion of the one-loop example carried out in the preceding paragraphs can easily be extended to a situation in which there is more than one pair of sewn Reggeons and, consequently, the group of automorphisms has more than one generator. To every pair of sewn Reggeons the preceding discussion of the integration region for fixed values of the surface parameters can be applied. The resulting general prescription is that every M loop dual amplitude is obtained as follows.

a) A set of closed boundary cycles is drawn on the sphere with M handles in such a way that they cut the surface into two symmetrical halves. This set is composed by at most $(M+1)$ boundary lines. We emphasize that there are sets with an arbitrary number of boundary lines ranging between 1 and $(M+1)$. This point will be clarified when we consider specific examples.

b) External variables are partitioned in all possible ways on the boundary lines. For each partition one must, in addition, consider all non-cyclic permutations of external variables on each boundary line.

c) All external variables are integrated on the surface along the closed boundary lines in such a way that their cyclic order is maintained and that every configuration on the surface is counted only once. This last requirement avoids the multiple counting that arises from the periodicity of the integrand.

d) Finally, one must integrate over all topologically equivalent but conformally inequivalent configurations of the Riemann surface described by the $(3M-3)$ surface parameters that give rise to different groups of automorphisms. We emphasize this point because the same group can be generated in many different ways or, equivalently, different generators can give rise to the same group. For example, the group generated by T_1 and T_2 and the one generated by T_1 and $T_2' = T_1^{-n} T_2 T_1^n$ are clearly the same, one is simply changing the identification of the generators. The multiplier is invariant under such a change, but the values of the invariant points (ξ_2, η_2) must not be allowed to cover the range of (ξ_2', η_2') because in that case one would clearly be multiple counting the configurations of the surface *). The second group of automorphisms would be naturally obtained if the sewing giving rise to T_2 were made on Reggeons implanted at the points $T_1^n(z)$ and $T_1^n(\tilde{z})$ instead of z, $\tilde{z}$ respectively; which are the same points on the surface. The restriction given in c) on the external variables, before the sewing is made, gives rise to the previous restriction on the invariant points of T_2.

---

*) We are grateful to Dr. E. Cremmer for a discussion of this point.

All these requirements imply that multipliers are such that their magnitude is between zero and one (if they are bigger than one, one is again multiple counting surface configurations) and that invariant points ξ_μ , η_μ are integrated on the unit circle in such a way that the cyclic order is maintained, and that they cover only once a fundamental region of the subgroup in which the corresponding generator T_μ has been eliminated. Some boundaries of the integration region correspond, as we shall discuss in more detail later on, to configurations in which there is a topological change on the surface, that is to say, when one or more handles vanish.

iv) The two-loop example

We shall illustrate here the general prescription with the two-loop example. The sphere with two handles is shown in Fig. 6a. The possible boundary sets which cut the surface into two symmetric parts are:

a) the three-boundary lines which come from an horizontal cutting of Fig. 6a; they are depicted in Fig. 6a and give rise to orientable amplitudes;

b) the two-boundary lines depicted in Fig. 6b; one of them cuts a Möbius strip from the double term and the other makes a hole in such a Möbius strip; this gives rise to a non-orientable amplitude;

c) the one-boundary line exhibited in Fig. 6c which leaves a double Möbius strip (two Möbius strips joined by a piece of boundary); this is a non-orientable two-loop diagram;

d) finally, the one-boundary line exhibited in Fig. 6d, which gives an orientable two-loop diagram with only one boundary, the so-called "pretzel" diagram that corresponds to one of the primitive operators of Gross et al.

When the corresponding group of automorphisms is considered, the different boundary sets will be related to different signs of the multipliers K_1 and K_2 and, eventually, to different orderings of the four invariant points ξ_1, η_1, ξ_2, η_2 on the unit circle. It is important to keep in mind that a hyperbolic generator $K>0$ determines two boundaries on the surface, and that a loxodromic generator $(K<0)$ determines only one, as discussed in the previous example. When both K_1 and K_2 are positive, the ordering of the invariant points on the unit circle is fixed for each amplitude. There are, therefore, two different amplitudes, corresponding to cases a) and d) given by

a) $K_1>0 \quad K_2>0 \quad \xi_1, \eta_1, \xi_2, \eta_2$

b) $K_1>0 \quad K_2>0 \quad \xi_1, \xi_2, \eta_1, \eta_2$

When one multiplier, say K_2, is negative, the relative position of ξ_1, η_1 with respect to ξ_2, η_2 is irrelevant for the same reason that in the one-loop non-orientable case the position of the external variables z_1 with respect to the invariant points is also irrelevant. Therefore, the non-orientable amplitudes b) and c) are specified only by

b) $K_1>0 \quad K_2<0$

c) $K_1<0 \quad K_2<0$

If we represent the isometric circles - with the corresponding invariant points inside - together with the invariant unit circle, we can have for a), b) and c) a pattern as that of Fig. 7. For d) the order of I_1^{-1} and I_2 on the unit circle must be interchanged. The relations between intersection points are given by

a) and d) $A_i' = T_i(A_i) \quad , \quad B_i' = T_i(B_i) \quad , i=1,2$

b) $A_1' = T_1(A_1) \, , \; B_1' = T_1(B_1) \, , \; A_2' = T_2(B_2) , \; B_2' = T_2(A_2)$

c) $A_i' = T_i(B_i) \quad , \quad B_i' = T_i(A_i) \quad , i=1,2$

For the configuration of Fig. 7, in which the isometric circles of the two generators T_1 and T_2 are external to each other, the isometric circles of the other transformations of the group are internal to the four basic isometric circles and, therefore, the region of the complex plane exterior to them represents the fundamental region.

The boundary sets are given by the following segments of the unit circle

a) $A_1' A_1$, $A_2' A_2$ and $B_1 B_2' + B_2 B_1'$

b) $A_1' A_1$, $B_1 B_2' + A_2 A_2' + B_2 B_1'$

c) $A_1' A_1 + B_1' B_2 + A_2' A_2 + B_2' B_1$

d) (We imagine I_1^{-1} and I_2 exchanged in Fig. 7)

$A_1' B_2' + B_2 B_1' + B_1 A_2 + A_2' A_1$

Let us remark that the "pretzel" diagram d) has some new features. Indeed, it can be thought as a sewing of a pair of Reggeons in a one-loop non-planar diagram. This one has two boundaries and - to obtain the "pretzel" - the two sewn Reggeons must belong to the two different boundaries. The sewing leaves us with the one-boundary pretzel, i.e., it decreased the number of boundary from two to one. Before the sewing, to transfer an external particle from one boundary to the other would imply different amplitudes, i.e., diagrams which are not related by a duality transformation. After the sewing has been done it is irrelevant from which of the non-dual configurations we had started.

The integration over the surface parameters implies the integration over one invariant point (three are fixed arbitrarily) and K_1 and K_2 (related to the radii of the circles) with the condition that $|K_\alpha| \leq 1$ where K_α is the multiplier of an arbitrary transformation T_α generated by T_1, T_2 and their inverses.

In varying the surface parameters two isometric circles corresponding to different generators can overlap. In this case some isometric circles of other T_α cease to be interior to the four basic isometric circles. A case corresponding to amplitude a) is visualized in Fig. 8, where the transformation to which the isometric circles belong is shown in the figure. The other isometric circles are interior to the ones plotted in the figure so that fundamental region is the part of the complex plane exterior to the shaded area. The boundaries, over which external variables are located, are now given by the arcs A_1A_1', A_2A_2' and $A_{12}A_{12}'$.

In the case under discussion all the transformations of the group are hyperbolic and in this case $K_\alpha = 1$ (T_α becomes parabolic) implies that the two conjugate isometric circles corresponding to T_α are tangent. Then, this configuration is a limit of the integration region over the $3M-3$ surface parameters. We shall see later on that this corresponds to a handle vanishing in the Riemann surface. Therefore we see from Fig. 8 that the integration region over K_1, K_2 and one of the invariant points is limited by [15]

$K_1 = 1$ ($A_1 = A_1'$ in Fig. 8)

$K_2 = 1$ ($A_2 = A_2'$ in Fig. 8)

$K_{T_1T_2} = K_{T_2T_1} = 1$ ($A_{12} = A_{12}'$ in Fig. 8)

Indeed, by using the expression for a multiplier of a product it is easy to show that $K_{T_1T_2} \leq 1$

$$| K_1 + K_2 + (\xi_1, \eta_2, \eta_1, \xi_2)(1-K_1)(1-K_2) | \geq 2\sqrt{K_1 K_2} \tag{2.24}$$

the equality sign of (2.24) being the limit of integration region corresponding to $K_{T_1T_2} = 1$.

The values of the three integration parameters for which $K_\alpha = 1 - T_\alpha$ different from T_1, T_2, T_1T_2 and T_2T_1 - are outside of the integration region [15]. This result is obtained by showing *) that the isometric circles I_α, I_α^{-1} of every T_α other than T_1, T_2, T_1T_2 and T_2T_1 are interior to conjugate isometric circles of one of the four transformations. Therefore, they cannot become tangent before conjugate isometric circles of the four transformations quoted become tangent and stop the integration.

A similar argument can be made for the set of orientable M loop diagrams with $(M+1)$ boundary lines, that include the planar diagram and some non-planar ones. In this case the pairs of isometric circles of T_μ and T_μ^{-1} $(\mu = 1,\ldots,M)$ are consecutive as in the two-loop case we have been considering. It is easy to see by application of the previous theorem that, if all pairs of isometric circles are exterior to one another, only the generators T_μ can become parabolic. When consecutive isometric circles of different generators overlap while keeping all their radii finite, it follows that the only new isometric circles that emerge into the fundamental region are those of $(T_1T_2\ldots\ldots T_M)$ and $(T_1T_2\ldots\ldots T_M)^{-1}$; the first one from inside

---

*) This can be done [15] by successive applications of the following theorem [11]. If I_1 and I_2^{-1} are exterior to each other, then I_{12} (the isometric circle of $T_{12} \equiv T_1T_2$) is contained in I_2.

$I_{T_M}^{-1}$ and the second one from inside $I_{T_1}^{-1}$. Since $I_{T_1T_2\ldots T_M}$ and $I_{(T_1T_2\ldots T_M)^{-1}}$ are now consecutive they can become tangent and the group element $T_1\ldots T_M$ can become parabolic. We find, therefore, $(M+1)$ parabolic points corresponding to the vanishing of the $(M+1)$ boundary cycles.

However, this is true when the radii of the isometric circles of the generators are kept finite. If the radius of I_μ and I_μ^{-1}, say is allowed to vanish first, either by letting $K_\mu \to 0$ or by letting $\xi_\mu \to \eta_\mu$ - which implies that the multipliers of other group elements vanish - then, an identical argument shows that $(T_1T_2\ldots T_{\mu-1}T_{\mu+1}\ldots T_M)$ can now become parabolic *). This can easily be understood in the sense that if the radius of I_μ is allowed to vanish first we have essentially an $(M-1)$ loop diagram and the new parabolic point is essentially the same than the one found before for the $(M-1)$ subloops. Therefore, altogether, we have (2^N-1) parabolic points although only $(M+1)$ can occur when all M handles are finite; the remaining ones occur only when one or more handles are allowed to vanish first by factorizing one or more Reggeons. However, all of them are in the domain of integration of the M loop amplitude we are considering.

d. <u>The Measure of Integration</u>

We have discussed the integration region by choosing as variables the $3M-3$ independent multipliers and invariant points of the transformations defining the group of automorphisms and the $N' = N-2M$ variables z_i that correspond to the external particles.

This choice is dictated from the explicit parametrization of the Green function V appearing in the integrand (2.10) [cf., Eq. (A.33)].

---

*) These results have been obtained independently by Kaku and Scherk [16].

This choice is also suited for the evaluation of the partition function and the determinant of the period matrix in the integrand of (2.10). Both depend only on the $3M-3$ surface variables. In the remaining factors of the measure of integration (volume element) we must still substitute the variables $z_\mu, \tilde{z}_\mu$ and x_μ by ξ_μ, η_μ and K_μ. In order to do this one must first substitute the variable x_μ by ρ_μ or $\hat{\rho}_\mu$ by using Eqs. (2.14) and (2.17). Then, one must perform a further change of variables from z_μ, $\tilde{z}_\mu$, ρ_μ (or z_μ, $\tilde{z}_\mu$, $\hat{\rho}_\mu$) to ξ_μ, η_μ, K_μ. This last step is easily done by taking for T_μ the first three (or last three) columns of Eq. (2.16) and writing it in terms of 2×2 matrices by using the general relation

$$\begin{bmatrix} a & b & c \\ \hat{a} & \hat{b} & \hat{c} \end{bmatrix} \equiv \begin{pmatrix} \gamma\hat{b}-\hat{a} & -\gamma a\hat{b}+b\hat{a} \\ \gamma-1 & -\gamma a+b \end{pmatrix} \tag{2.25}$$

where

$$\gamma = \frac{(b-c)(\hat{a}-\hat{c})}{(a-c)(\hat{b}-\hat{c})} \tag{2.26}$$

Finally, K_μ, ξ_μ and η_μ can be easily written in terms of the 2×2 matrix elements by using well-known relations [see, for example, Eq. (B.1) of Appendix B].

These straightforward algebraic manipulations are particularly simple for the M loop planar amplitude, which is obtained by sewing with a twisted propagator M pairs of consecutive Reggeons (M planar tadpoles). In this case each T_μ is given by Eq. (2.20) and the invariant points and multipliers by Eqs. (2.21) and (2.22). The Jacobian for the change of variables to invariant points and multipliers is given by Eq. (2.23). Moreover, the duality properties of the M loop planar amplitude - which are automatic in our formulation - allows us to choose arbitrarily the relative positions of

external scalars and tadpoles. When all external particles are chosen to be consecutive, the M loop formula can be written

$$A^{\text{planar}}_{M,N'} = \int \frac{1}{dV_{abc}} \frac{\prod_{i=1}^{N'} dz_i}{\prod_{i=1}^{N'} (z_{i+1}-z_i)^{1+\alpha}} \prod_{\mu=1}^{M} \frac{dK_\mu d\xi_\mu d\eta_\mu (y_{\mu-1}-y_\mu)}{K_\mu(1-K_\mu)(\xi_\mu-\eta_\mu)(y_{\mu-1}-\xi_\mu)(y_{\mu-1}-\eta_\mu)} \times$$

$$\times \left[\frac{y_{\mu-1}-\eta_\mu}{\eta_\mu-y_\mu}\right]^{a} \exp -\frac{1}{2}\sum_{i,j} p_i\cdot p_j\, V(z_i,z_j;z_0,z_0') \qquad (2.27)$$

where

$$y_\mu \equiv T_\mu\left[T_{\mu-1}\left[\cdots\left[T_1(z_1)\right]\right]\right]$$

$$y_0 \equiv z_1 \quad , \quad z_{N'+1} \equiv y_M \qquad (2.28)$$

Let us now compare our result with the one given by Kaku and Yu [3] for the planar case. These authors do not integrate over the loop momenta, but it is quite easy to undo the loop momentum integration in our case (see Appendix A). One finds [2] that the terms raised to the power $p_i\cdot p_j$ are exponentials of third Abelian integrals in the complex normalization, and that terms raised to the power $p_i k_\mu - k_\mu$ being a loop momentum - are exponentials of first Abelian integrals. Using the Poincaré ϑ series the third Abelian integral can be written in the form of an infinite product [2] which is, of course, the same as the one given by Kaku and Yu [3]. The comparison of the first Abelian integrals is more delicate because the Poincaré ϑ series gives them as a series of logarithmic singularities at the centres of the isometric circles of the elements of the group [see Eq. (A.30)] which do not lie on the unit circle. However, as shown by Burnside [12], these logarithmic singularities cancel and the first Abelian integrals are singular only at the invariant points of the group, that lie on the unit circle. This phenomenon is what Kaku and Yu [3] call the "infinite cancellation technique".

The measure of integration is the same, as for a factor we shall discuss later, if one interprets their result [Eq. (10) of Ref. 3)], as valid only in configurations in which one never has adjacent tadpoles. The extra factor

$$\prod_{\mu=1}^{m}(1-K_\mu) \tag{2.29}$$

they have as compared to the result displayed in (2.27) is probably related to gauge factors in the N Reggeon vertex and is reminiscent of the factor that appeared in the single-loop formula when spurious states were eliminated from the closed loop [9]. Indeed, it is quite straightforward to check that, because of the properties of Olive's vertex, we do have spurious states propagating in our one-loop planar formula. In this case, having only one generator, it is clear that a factor (1-K) will never spoil the duality properties of the amplitude. For more than one loop, there are duality transformations that correspond to sewing the diagram in a different way and that amount to changing the generators of the group and using, for example, T_1 and T_1T_2 as generators instead of T_1 and T_2. Since the multiplier of T_1T_2 is a function of the multipliers and invariant points of T_1 and T_2, the factor (2.29) is not a dual invariant factor by itself.

Let us discuss briefly the results we would have obtained if the Lovelace N Reggeon vertex [7] had been used at the place of (2 3) in our calculations. Lovelace vertex is obtained by (2.3), (2.9) by replacing every β_μ by z_μ. The multiloop amplitude is then given by Eq. (2.10) with β_μ substituted by z_μ.

For every pair of sewn Reggeons (with variables z_μ and $\tilde{z}_\mu$) one can introduce two variables β_μ and $\tilde{\beta}_\mu$ related to x_μ by an equation as (2.14) in which $\beta_{\mu-1}$ and $\tilde{\beta}_{\mu-1}$ are substituted by $z_{\mu-1}$ and $\tilde{z}_{\mu-1}$ respectively. The integration over $d x_\mu$ can be again eliminated by (2.17) in terms of $d\beta_\mu$ or $d\tilde{\beta}_\mu$. The generators of the group of automorphism are again given by (2.16) with $\beta_{\mu-1}$ and $\tilde{\beta}_{\mu-1}$ replaced by $z_{\mu-1}$ and $\tilde{z}_{\mu-1}$. This implies that the z and β variables appearing in the measure have different expressions in terms of invariant points and multipliers.

In the planar case, for instance, the relation between the z and β tadpole variables with invariant points and multiplier would be

$$\xi_\mu = z_{\mu+1} \quad , \quad K_\mu = -(\beta_\mu, z_\mu, z_{\mu+1}, z_{\mu+2}) = (z_\mu, \eta_\mu, z_{\mu+1}, z_{\mu+2}) \tag{2.30}$$

instead of Eqs. (2.21), (2.22). For the multiloop planar amplitude, the modification to (2.27), implied by the use of the Lovelace vertex is simply an extra factor

$$\prod_{\mu=1}^{n} (1 - K_\mu)$$

in the integration measure, factor we have already discussed. We remark that due to the operatorial duality of the vertex [8] (2.3), the unintegrated multiloop amplitudes satisfy duality relations. The drawback of our procedure is that we have spurious states propagating in untwisted lines. In the approaches in which spurious states are eliminated through the projection operator, duality relations hold only for integrated amplitudes. However, we have understood that the integration region is not the one given by the operatorial prescription due to periodicities, and this is why it is so relevant, in our point of view, to have duality for unintegrated expressions.

3. SINGULARITIES OF MULTILOOP AMPLITUDES

The purpose of this Section is to investigate the singularities of multiloop amplitudes. We have seen in the previous section that the multiloop formula involves the integration of the exponential of the Green function of a sphere with M handles in two steps. For a given configuration of the surface the variables associated with the external particles are integrated along closed cycles. In addition, one must integrate over all conformally non-equivalent configurations of the surface. The Green function $V(z_i, z_o; z_j, z'_o)$ depends explicitly on the Koba-Nielsen variables of external particles, and, implicitly, on the $(3M-3)$ Riemann moduli that describe the conformally non-equivalent configurations of the surface. Beside the obvious logarithmic singularities that occur whenever z_i and z_j coincide, the Green function can also exhibit logarithmic singularities in its dependence on the surface parameters. Indeed, the integration limit in the surface parameters represents configurations in which the surface changes its topology. The sphere with M handles looses there one or more handles. We will first discuss the general features of these end point singularities and then show explicitly how general methods of domain variational theory [5] can be used in order to evaluate them.

The multiloop amplitude exhibits in general two elementary classes of singularities. The first one, which we will call unitarity singularities, occurs when some multiplier K_α vanishes. The second one, for which some K_α reaches the value $+1$ or -1, gives rise to singularities, or divergencies, which are not related to unitarity and which are a specific characteristic of dual theories. As we will see later on, both cases represent situations in which the surface looses a handle. Of course, several singularities can occur simultaneously, giving rise to the vanishing of more than a handle.

a. Unitarity Singularities

Let us first discuss the end point $K_\mu = 0$ in which K_μ is the multiplier of one of the generators used to define the group of automorphisms and which appear as one of the $3M-3$ explicit variables of the surface.

In this case the radius of the corresponding isometric circles shrinks to zero with K_μ. In the two-loop case of Fig. 7, for instance, we would find the two isometric circles I_1 and I_1' (if $K_1 \approx 0$) shrinking around the two fixed points ξ_1 and η_1. Then, the external variables z_1, which lie on the arcs described before can become arbitrarily close to the fixed points in question. When this happens, the function $\phi_\mu(z_i)$ appearing in the expression (A.33) of the Green function develops a logarithmic singularity [5),12)] of the form $\log(z_i - \xi_1)$ which goes as $\frac{1}{2}\log K_1$ if z_i approaches the isometric circle. This is, however, not sufficient to give a singularity of the amplitude due to the fact that $(A^{-1})_{\mu 1}$ behaves as $(\log K_1)^{-1}$, and the logarithmic behaviour is, therefore, cancelled. But if two external variables z_i and z_j approach the isometric circle, then we will find a term coming from

$$e^{-\frac{\alpha'}{2} p_i p_j \phi_1(z_i)(A^{-1})_{11}\phi_1(z_j)} \simeq e^{-\frac{\alpha'}{2} p_i p_j \frac{\log|z_i-\xi_1|\ \log|z_j-\xi_1|}{\log K}} \tag{3.1}$$

The term containing the third Abelian integral in the complex normalization, $\langle z_i | \Gamma (1-\Sigma)^{-1} | z_j \rangle$, in Eq. (A.33) is regular when z_i or z_j approach the invariant point. However, if z_i and z_j approach the invariant point from the same side of the isometric circle - as it happens for the planar case, for example, then the third Abelian integral gives the usual Reggeon pole when $z_i \to z_j$. In this case, the integration over z_i, z_j and K_1 gives poles in the variable $p_i \cdot p_j$ with numerator functions that have cuts in the same variables coming from the term in the integrand given by Eq. (3.1).

If z_i and z_j approach the invariant point from opposite sides of the isometric circle, as it happens for non-planar diagrams, the integration over z_i, z_j and K_1 gives rise only to a cut, as expected. This cut is the one associated with the Reggeon-Reggeon cut dual to the Pomeranchuk-like singularity [14),17)] we shall discuss later on.

The origin of the unitarity cuts is easy to understand. Indeed, they come from the first Abelian integral contribution to the Green function which arose [1),2)] from the integration over the loop momentum.

Had we analyzed the $K_\mu \sim 0$ contribution before integrating over the loop momentum we would have recognized that it corresponded to an unsewn Reggeon implanted, with the loop momentum k_μ and $-k$, at the two invariant points ξ_μ and η_μ, respectively. We would have found only poles in the square of the momenta containing k; the pinching of these poles on the integration contour over k_μ being responsible, as in the usual Feynman diagrams, of the cuts.

From the point of view of the surface, the $K_\mu \sim 0$ can be visualized as a handle becoming infinitely thin and, therefore, disappearing. The handle is the one which has $C_{2\mu}$ as the associated "vertical" cycle in Fig. 2. The analysis of the singularities is particularly easy in this case due to the fact that the variable which goes to zero is a multiplier of one of the generators that appears explicitly in the expression for the Green function. But, of course, multipliers K_α of other members of the group of automorphisms can vanish in the boundary of the 3M-3 variable integration. In the two-loop case discussed before, we had as independent variables, two multipliers (K_1, K_2) and one invariant point (say ξ_1). The integration region has as boundaries not only $K_1 = 0$ and $K_2 = 0$ but also $\xi_1 = \eta_1$ (with K_1 arbitrary). It is easy to show that this implies $K_{12} = 0$, which corresponds to the vanishing of the handle which separates the two holes of the double torus of Fig. 6a. Here, the parameter that goes to zero in the limit in which the surface changes is not one of

the variables explicitly used in the construction of the Green function. However, the logarithmic singularity in terms of such a parameter can always be exhibited by using the classical results of domain variational theory [5]. Then one must find the explicit relation between that parameter and some of the $(3M-3)$ independent variables that have been chosen. We shall illustrate later on this procedure. We turn now to the discussion of the singularities appearing in the $|K_\alpha| \sim 1$ limit which, as discussed before, are also boundaries of the integration region.

b. Parabolic Singularities

We have seen in the previous section that whenever a multiplier goes to zero there is a handle that vanishes in our sphere with M handles. This behaviour at the end point of the region of integration gives rise to the normal threshold or Regge cuts in the multiloop amplitude, and is visualized by thinking of some of the handles of Fig. 2 becoming very thin and finally breaking down. However, this is not the only way in which a handle can vanish. We can also think that the handle becomes so thick that finally the open space in the middle disappears. When such a thing happens, an "internal boundary line" shrinks to a point. This means, in the language of the group of automorphisms obtained by cutting the surface along the $C_{2\mu-1}$ cycles (the one that we discussed in Section 1) that the arc of the unit circle between the isometric circles of the generator associated with the handle tends to a point, that is to say, the two isometric circles become tangent and the generator becomes parabolic. Therefore, parabolic points, which are in the boundary of our region of integration, also correspond to the vanishing of a handle in our Riemann surface. If our closed Riemann surface were sliced "horizontally" to obtain two copies of an open Riemann surface with $(N+1)$ boundaries (the original Riemann surface of the analogue model) we would observe that a handle vanishing in the way we are describing now would correspond to a hole shrinking to zero in the open Riemann surface. This explains the connection with the more familiar surfaces of the analogue model.

We shall, however, pursue our discussion in the next section in terms of the Green function of the sphere with handles because, as explained before, this is the approach that can be extended to more general situations. Before doing that we shall briefly review some classical results of domain variational theory [5].

c. Results from Domain Variational Theory

We shall use here the notation of Schiffer and Spencer [5] and denote the Green function of a sphere with M handles by $V(t,t_o;q,q_o)$ where t's and q's are points on the surface. We shall keep the notation z_i, z_j for the case in which we explicitly represent these invariant functions on the surface in terms of automorphic functions in the complex plane.

Consider a sphere with M handles, to be denoted by $\mathcal{M}$. Let us pick up two points on the surface, q_1, q_2 and consider the Green function $V(t,t_o;q_1,q_2)$ where t_o is some unessential parameter point, fixed on the surface once and for all. When t is near q_1 $V(t,t_o;q_1,q_2)$ behaves like $\log\{|t-q_1|^{-1}\}$; and when t is near q_2 it behaves like $\log|t-q_2|$. Therefore, one can define two closed curves γ_1, γ_2 around q_1, q_2 respectively by

$$\gamma_1 : \quad V(t,t_o;q_1,q_2) = \log\frac{1}{\epsilon} \tag{3.2}$$

$$\gamma_2 : \quad V(t,t_o;q_1,q_2) = \log\epsilon \tag{3.3}$$

where ϵ is a small parameter. An extra handle is attached to the surface by cutting two holes along the profile cycles γ_1, γ_2 and identifying the two boundaries in a suitable way. The part $\mathcal{M}$ outside γ_1, γ_2 becomes $\mathcal{M}^*$, a sphere with $(M+1)$ handles (see Fig. 9). The only reason to cut the holes along profile lines of the Green function is to simplify the analysis that follows.

In order to identify the curves γ_1 and γ_2 it is convenient to introduce the analytic function

$$\nu(t,t_o;q_1,q_2) = \Omega_{q_1q_2}(t) - \Omega_{q_1q_2}(t_o) \tag{3.4}$$

in such a way that

$$V(t,t_o;q_1,q_2) = \mathrm{Re}\,\nu(t,t_o;q_1,q_2) \tag{3.5}$$

Let us now choose two arbitrary points $t_1^{(o)}$ and $t_2^{(o)}$ on γ_1 and γ_2, respectively, that we wish to identify. Then, we can write

$$\nu(t_1^{(o)},t_o;q_1,q_2) = \nu(t_2^{(o)},t_o;q_1,q_2) + 2\log\frac{1}{\varepsilon} - i\alpha \tag{3.6}$$

where α is a real constant because it follows from Eqs. (3.2) and (3.3) that Re v jumps by $2\log 1/\varepsilon$ when going from γ_1 to γ_2. Then, starting from $t_1^{(o)}$ and $t_2^{(o)}$ we identify points $t_1 \in \gamma_1$ and $t_2 \in \gamma_2$ if they satisfy the equation

$$\nu(t_1,t_o;q_1,q_2) = \nu(t_2,t_o;q_1,q_2) + 2\log\frac{1}{\varepsilon} - i\alpha \tag{3.7}$$

that is to say, points in γ_1 and γ_2 are identified by keeping constant the imaginary part of the change in v in going from γ_1 to γ_2. This has as an immediate consequence that if t_1 moves around γ_1 in the clockwise sense, t_2 moves around γ_2 in the counter-clockwise sense. The reader will easily convince himself that this is exactly what is needed in order to obtain a handle from the identification of the two holes.

The region in $\mathcal{M}$ outside the two curves γ_1 and γ_2 becomes a sphere with $(M+1)$ handles, $\mathcal{M}^*$, after the identification is made. We shall denote by $V^*(t\,t_o, q\,q_o)$ the Green function of $\mathcal{M}^*$. Following this procedure one can add an arbitrary number of handles to $\mathcal{M}$ in order to get a new surface $\mathcal{M}^*$.

An exact integral equation can be written in order to compute V^* from the knowledge of V, when the two surfaces differ by an arbitrary number of handles. Rather than writing here this integral equation, we shall give an iterative solution given by Schiffer and Spencer which will be the basis of most of our discussions. If $\mathcal{M}^*$ and $\mathcal{M}$ differ by one handle, then we have

$$V^*(t,t_0;q,q_0) = V(t,t_0;q,q_0) + \frac{1}{2\log\varepsilon} V(t,t_0;q_1,q_2)\,V(q,q_0;q_1,q_2) +$$

$$+ 4\varepsilon^2 \mathrm{Re}\left\{ e^{i\alpha} \frac{\partial V(qq_0;q_1,q_2)}{\partial q_1} \frac{\partial V(tt_0;q_1,q_2)}{\partial q_2} + \right.$$

$$\left. + e^{i\alpha} \frac{\partial V(qq_0;q_1,q_2)}{\partial q_2} \frac{\partial V(tt_0;q_1,q_2)}{\partial q_1} \right\} + O(\varepsilon^3) \qquad (3.8)$$

This equation gives the behaviour of $V^*(t\,t_0;q\,q_0)$ when the handle vanishes, that is to say, when $\varepsilon \to 0$, in terms of the Green function of the surface without the handle.

We shall often be interested in analyzing the behaviour of the Green function when several handles vanish simultaneously. Here the main point is that, as shown by Schiffer and Spencer [5], the behaviour of V^* is additive in the number of handles up to and including the quadratic terms in ε. In other words, if h handles vanish, V is now the Green function of the surface with h less handles and one has to add h terms similar to the one exhibited in Eq. (3.8), depending on the parameters of each handle. The error goes to zero faster than $\varepsilon_i \varepsilon_j (i,j = 1,\ldots,h)$, and this simple observation will be sufficient for our purposes. Finally, we remind the reader that the multiloop integrand in Eq. (2) contains the regular part of the Green function if the index $i = j$. Subtracting $\log|t-q|$ on both sides of Eq. (3.8) we see that when $V^*(t,t_0;q,q_0)$ is replaced by its regular part, the net effect is to replace $V(t,t_0;q,q_0)$ by its regular part in the right-hand side of the equation. There is no restriction imposed, when $i = j$, to the ε dependent terms of the variational formula. We now proceed to apply Eq. (3.8) to the analysis of singularities and divergencies of multiloop amplitudes.

d. Parabolic Singularities and Renormalization

We have previously discussed in some detail the unitarity singularities coming from $K_\alpha \to 0$. We mentioned, however, that apart from the simplest cases $K_\mu \to 0$ (i.e., a vanishing multiplier corresponding to a generator of the group of automorphisms) in which the singularities were evident, the general method to investigate them is to apply domain variational theory. This amounts to using the results of the previous section and relating the relevant surface parameter ε to some of the $(3M-3)$ surface integration parameters, multipliers and invariant points of the generators, in terms of which the measure of integration is given and, in particular, to the partition functions which, to the best of our knowledge, is not an invariant function on the surface.

This last step is particularly evident for the singularities arising from $|K_\alpha| \to 1$. In this case, the small parameter ε whose zero limit implies the vanishing of a handle, must be related to a multiplier going to one. As discussed in the last section, the vanishing of the handle is related to the vanishing of a hole if the surface is cut along the "horizontal" $C_{2\mu}$ canonical cycles. In principle, one could construct a new group of automorphism by cutting the surface along the even or "horizontal" $C_{2\mu}$ canonical cycles. The Green function, being an invariant function on the surface, is, of course, independent of the way in which the surface is parametrized; but one still needs to relate the new surface parameters to the parameters of the measure, which is given explicitly in terms of the parameters of the group corresponding to the "vertical" cutting. However, the generators of the new group are highly non-linear functions of the generators of the old one [5),18)], and, to the best of our knowledge, these functions are not known in general. Therefore, we cannot at the moment rewrite globally the measure in a more suitable way.

In the one-loop case, the change from a "vertical" to a "horizontal" group of automorphisms corresponds to performing Jacobi's imaginary transformation [19)] on the θ functions, as done first by

Neveu and Scherk [20]. We have emphasized before that in the multiloop case the corresponding change of variables is not explicitly known. We have circumvented this problem by carrying out a "local" change of variables which is not valid everywhere but only near the end points where the loop amplitude diverges, using domain variational theory. This is sufficient to obtain the most singular part of the multiloop integrand and define, if desired, suitable counter-terms.

We shall illustrate the method by investigating the $K_\alpha \to 1$ singularity and divergence in an orientable N loop diagram with $(N+1)$ boundary lines. We will start by discussing the well-known case of the single-loop diagrams in order to motivate our approach to the more general case.

i) The one-loop case

We shall consider the case of orientable diagrams, in which we have two boundary lines on the torus, as shown in Fig. 4. If the torus is sliced horizontally, we get two copies of an annulus, the original open surface of Nielsen's analogue model.

The group of automorphism corresponding to single-valued functions on a torus has only one generator. Consider the group obtained by cutting the surface along the vertical cycle C_1; and let us call T its generator, which is written as

$$\frac{T(z)-\xi_1}{T(z)-\xi_2} = K\,\frac{z-\xi_1}{z-\xi_2} \tag{3.9}$$

As it is explained at length in I, going in the complex z plane around the isometric circle I_t of T is equivalent to going around the C_1 cycle on the surface, and going in the complex plane from a point z to its homologous $T(z)$ corresponds to going around the C_2 cycle on the surface. In

particular, if z is on I_t, $T(z)$ is on I_t^{-1}. In this case, there is only one first Abelian integral, given by

$$\phi(z) = \frac{1}{2\pi i} \log\left[\frac{z-\xi_1}{z-\xi_2}\right] \tag{3.10}$$

and whose periods are easily calculated

$$P_{C_1} = 1 \tag{3.11}$$

$$P_{C_2} = B = \frac{\log K}{2\pi i} \tag{3.12}$$

We remind the reader that first Abelian integrals in the complex normalization are uniquely defined once all the periods $P_{C_{2\mu-1}}$ are given. The remaining periods, which determine the period matrix $B_{\mu\nu}$, can in principle be calculated. Therefore, Eq. (3.11) is just the normalization condition for $\phi(z)$.

Let us now imagine that we represent single-valued functions on a torus by means of another group of automorphisms that would correspond to cutting the surface along the horizontal cycle C_2. We shall denote the new generator by $\bar{T}$, given by

$$\frac{\bar{T}(z') - \eta_1}{\bar{T}(z') - \eta_2} = \rho \frac{z' - \eta_1}{z' - \eta_2} \tag{3.13}$$

but now the role of the C_1 and C_2 cycles has been interchanged: going around $I_{\bar{T}}$ is equivalent to going around the C_2 cycle on the surface, and going from z' to $\bar{T}(z')$ is equivalent to going around the C_1 cycle. We now compute the first Abelian integral,

$$\bar{\phi}(z') = \frac{1}{\log\rho} \log\left[\frac{z'-\eta_1}{z'-\eta_2}\right] \tag{3.14}$$

which is correctly normalized because

$$P_{C_1} = 1 \tag{3.15}$$

and the remaining period is given by

$$P_{C_2} = B = -\frac{2\pi i}{\log \rho} \tag{3.16}$$

The two functions ϕ and $\tilde{\phi}$ are two different representations of the same invariant function on the torus. But, if this is so, the period B must be the same, so from Eqs. (3.12) and (3.16) we get

$$\log K = \frac{4\pi^2}{\log \rho} \tag{3.17}$$

which establishes the relation between the generators of the "horizontal" and the "vertical" groups of automorphisms. Using the fact that $\rho = R^2$, where R is the radius of the annulus (this comes from the fact that the torus is the double of the annulus, as discussed at length in I) we recognize Eq. (3.17) as the change of variables required by the Jacobi transformation used by Neveu and Scherk [20] to investigate the single-loop divergence.

ii) The multiloop case

The previous example shows how to proceed in the more general case. The sphere with one handle depends on only one Riemann modulus (the multiplier of the generator of the group) and the relation between different parametrizations of the surface is given by the period B. In general, it is known that the M×M period matrix $B_{\mu\nu}$ are continuous functions of the (3M-3) Riemann moduli that characterize the surface.

The relation between different parametrizations of the surface can in principle be obtained in the same way as before by computing the period matrices and demanding that they be equal. This procedure gives a set of (3M-3) Riemann moduli as implicit functions of the other set, because it can also be shown that there are only (3M-3) independent matrix elements of the period matrix [18].

However, as soon as one goes beyond the one-loop problem, it is no longer possible to compute explicitly the period matrix. As said before, we have circumvented this problem by computing the period matrix B only near the point when a handle vanishes, using domain variational theory. We shall, therefore, derive a suitable change of variables for the multi-loop amplitude that will not be correct "globally", as Eq. (3.17) was, but only "locally", near the end-points of the integration region where the multiloop integral diverges. This will be sufficient in order to obtain the most divergent part of the amplitude and define suitable counter-terms.

The Riemann surface associated with the M loop amplitude is parametrized in terms of the generators of the group of automorphisms. Three invariant points can be kept fixed because of the projective invariance of the multiloop formula, and the remaining invariant points and multipliers provide a natural set of 3M-3 Riemann moduli. Let us assume that one of the generators, say, T_M, becomes parabolic. In Appendix B the period matrix is estimated near the parabolic point and it is shown that

$$B_{MM} = \frac{\log K_M}{2\pi i} + O(\delta^2) \quad ; \delta \sim 1 - K_M \tag{3.18}$$

and that all the remaining matrix elements vanish like δ^2.

In order to describe the vanishing of the handle in terms of domain variational theory, we must proceed as indicated in Fig. 9. The two circles γ_1 and γ_2 along which the holes are cut will become, when identified, an even canonical cycle C_{2M}. An arc going from a point $t_1^{(o)}$ in γ_1 to its homologous $t_2^{(o)}$ in γ_2 will become an odd cycle C_{2M-1}. If we compare with what we did for the normal threshold cut, it is clear that the roles of the even and odd cycles associated with the vanishing handle have been interchanged. Equation (3.8) gives at once the behaviour of the momentum-dependent part of the Veneziano integrand in this parametrization, but we must still find the behaviour of the measure of integration when $\varepsilon \to 0$. A relation between K_M and ε will be found by estimating the behaviour of the period matrix as $\varepsilon \to 0$ and comparing with Eq. (3.18).

Once the variation of the Green function is known several useful functional relations given by Schiffer and Spencer [5] allow one to calculate the behaviour of all the other functionals that can be defined on the Riemann surface like, for example, first Abelian integrals and period matrices. We shall estimate, however, the period matrix element B_{MM} in a more direct way. The first problem is to compute $\phi_M^*(t)$. An excellent candidate is the function

$$\psi(t) = c\left[\omega_{q_1 q_2}(t) - \omega_{q_1 q_2}(t_0)\right] \tag{3.19}$$

where $\omega_{q_1 q_2}(t)$ is the third Abelian integral in the complex normalization of the surface $\mathcal{M}$ corresponding in this case to the sphere with $(M-1)$ handles. Indeed, the function $\psi(t)$ is regular in $\mathcal{M}^*$ (remember that q_1 and q_2 are in $\mathcal{M}$ but not in $\mathcal{M}^*$). Moreover, third Abelian integrals in the complex normalization have no periods around the odd cycles $C_{2\mu-1}$, $\mu = 1,\ldots,M-1$. Since the first $(M-1)$ canonical cycles of $\mathcal{M}$ and $\mathcal{M}^*$ coincide, we conclude that $P_{C_{2\mu-1}}(\psi) = 0$, for $\mu = 1,\ldots,M-1$. Therefore, if we can fix

the constant C in such a way that $P_{C_{2\mu-1}}(\psi) = 1$, $\psi(t)$ will become our first Abelian integral $\phi^*_M(t)$. Using the relation between third Abelian integrals in the real and the complex normalization, Eq. (3.19) can be rewritten as

$$\psi(t) = C\left\{\Omega_{q_1q_2}(t) - \Omega_{q_1q_2}(t_o) + \sum_{\mu=1}^{M-1} \alpha_\mu \left[\phi_\mu(t) - \phi_\mu(t_o)\right]\right\} \tag{3.20}$$

where the coefficients α_μ are explicitly given in I but are irrelevant for our purposes here. In order to compute $P_{C_{2M-1}}(\psi)$ we must investigate how $\psi(t)$ changes when going from a point t_2 on γ_2 to its homologous t_1 on γ_1. The change in the function $[\Omega_{q_1q_2}(t) - \Omega_{q_1q_2}(t_o)]$ is immediately obtained from Eqs. (3.4) and (3.7)

$$\Omega_{q_1q_2}(t_1) - \Omega_{q_1q_2}(t_2) = -2\log\varepsilon - i\alpha$$

and the remaining part of the right-hand side of Eq. (3.20) contributes a complex constant plus terms linear in ε because the $\phi_\mu(t)$ $(\mu = 1,\ldots,M-1)$ are the first Abelian integrals of $\mathcal{M}$, and are consequently regular at the points q_1, q_2. Then, we conclude that

$$P_{C_{2M-1}}(\psi) = -C\left[2\log\varepsilon + \beta + O(\varepsilon)\right]$$

where β is a complex constant. Then,

$$\phi^*_M(t) = -\frac{1}{2\log\varepsilon + \beta + O(\varepsilon)}\left[\omega_{q_1q_2}(t) - \omega_{q_1q_2}(t_o)\right] \tag{3.21}$$

Now, the matrix element B_{MM} is easily obtained. Since $\omega_{q_1q_2}(t)$ has period $2\pi i$ when going around γ_1 (it has a logarithmic singularity at $t = q_1$), we obtain

$$B^*_{M,M} = -\frac{i\pi}{\log\varepsilon + \beta' + O(\varepsilon)} \tag{3.22}$$

From Eqs. (3.18) and (3.22) we obtain

$$\log K_M + O\left[(1-K_M)^2\right] = \frac{2\pi^2}{\log\varepsilon + \beta' + O(\varepsilon)} \tag{3.23}$$

so we conclude that, near $\varepsilon \to 0$, the multiplier behaves like

$$\log K_M = \frac{2\pi^2}{\log\varepsilon} + O\left[(\log\varepsilon)^{-2}\right] \tag{3.24}$$

Using Eq. (3.24) to perform a change of variables in the partition function that diverges when $K_M \to 1$, as done in the one-loop case, one easily finds

$$\frac{dK_M}{\prod_{n=1}^{\infty}(1-K_M^n)} \simeq \varepsilon^{-\frac{4}{3}}\, d\varepsilon \qquad \text{when } \varepsilon \to 0 \tag{3.25}$$

This behaviour is the same as the one found in the one-loop case. All the manipulations done in this section were necessary only to establish that the parameter ε that occurs in Eq. (3.25) is the same as the one that parametrizes the behaviour of the Green function in Eq. (3.8). The results of domain variational theory for the Green function can now be combined with the behaviour of the partition function to investigate the divergence of multiloop amplitudes.

iii) Analysis of divergencies

Let us first consider a planar diagram, with (N+1) boundary lines. Before getting involved in the analysis of all possible simultaneous singularities, we shall complete the previous discussion and consider the behaviour of the loop integrand when only one generator becomes parabolic. In particular, we are interested in the term of V^* that has the dependence on $\log\varepsilon$

$$\exp\left\{-\frac{1}{2}\sum_{i,j} p_i p_j \frac{1}{2\log\varepsilon} V(q_i q_0; q_1 q_2)\, V(q_j q_0'; q_1 q_2)\right\} \tag{3.26}$$

where q_i, q_j are the variables associated with external particles and are integrated along the boundary lines as discussed in Section 2. We emphasize here that V in Eq. (3.26) is the Green function of the sphere with $(M-1)$ handles, which is divided in two symmetric halves by M boundary lines. When the new handle is attached and a new boundary line is drawn on the surface, one must proceed in such a way that the new surface $\mathcal{M}^*$ is again symmetric and can be divided into two halves by cutting it along the $(M+1)$ boundary lines. This is easily achieved by cutting the two holes along cycles γ_1 and γ_2 that are symmetric with respect to the remaining M boundary lines. When the two cycles γ_1 and γ_2 are identified to construct $\mathcal{M}^*$, they will become the new boundary line on the sphere with M handles. For the two circles to be symmetric, they must be cut around symmetric points q_1, q_2 with respect to the M boundaries of $\mathcal{M}$; or, in other words, q_2 must be equal to $\tilde{q}_1$, the conjugate point of q_1 on $\mathcal{M}$ with respect to the M boundary lines that we have on this surface.

Using momentum conservation, we can get rid of the q_0, q_0' dependence in Eq. (3.26) and write it as:

$$\exp\left\{-\frac{1}{2}\sum_{i,j} p_i p_j \frac{1}{2\log\varepsilon} \mathrm{Re}\,\Omega_{q_1\tilde{q}_1}(q_i)\, \mathrm{Re}\,\Omega_{q_1\tilde{q}_1}(q_j)\right\} \tag{3.27}$$

Let us now pause for a moment to consider one of the two identical surfaces obtained by cutting $\mathcal{M}$ horizontally along the boundary lines. Its Green function is defined in terms of the third Abelian integral of the original surface $\mathcal{M}$ as [5]

$$G(q',q) = \frac{1}{2}\left\{\Omega_{q\tilde{q}}(q') - \Omega_{q\tilde{q}}(\tilde{q}')\right\} \tag{3.28}$$

and it vanishes on the boundaries simply because, on the boundaries, conjugate points coincide. It is shown in Ref. 5) that $G(q',q)$ can be rewritten as

$$G(q',q) = R_4\,\Omega_{q\tilde{q}}(q') + C \tag{3.29}$$

where C is a constant independent of q'. Therefore, momentum conservation allows us once again to rewrite Eq. (3.27) as

$$\exp\left\{-\frac{1}{2}\sum_{i,j} p_i p_j \frac{1}{2\log\varepsilon}\, G(q_i,q_1)\, G(q_j,q_1)\right\} \tag{3.30}$$

and, therefore, we can immediately conclude that the coefficient of $\log(1/\varepsilon)p_i p_j$ vanishes whenever one or the two particles of momentum p_i, p_j are implanted on a boundary line of $\mathcal{K}$, that is to say, on a boundary that is not shrunk to zero by the handle that vanishes. The only problem that remains is to consider the case in which the two particles i and j are inserted in the boundary that goes to zero with the handle. This is most easily seen directly from Eq. (3.26), because $V(q_i,q_o;q_1,q_2)$ just cancels the $\log\varepsilon$ in the denominator if q_i is on γ_1, due to Eq. (3.2). On the other hand, $V(q_j,q_o';q_1,q_2)$ is not identically equal to $\log\varepsilon$ if q_j is on γ_1 because $q_o' \neq q_o$, but we can replace it by $\log\varepsilon$ because, in any case, Eq. (4.18) is independent of q_o and q_o'. Therefore, the final result is that we can rewrite Eq. (3.26) as

$$\exp\left\{-\frac{1}{2}\sum_{i,j}{}' \frac{1}{2} p_i p_j \log\varepsilon\right\} \tag{3.31}$$

where the sum $\sum'$ extends only to the particles attached to the vanishing boundary. Putting together Eqs. (3.25) and (3.31) we see that the integrand behaves near $\varepsilon = 0$ as

$$\varepsilon^{-\left(\frac{4}{3}+\frac{\bar{s}}{2}\right)} \tag{3.32}$$

where $\bar{s}$ is the invariant mass of the particles entering into the vanishing boundary line. This behaviour gives rise to the same Pomeranchuk-like singularity found in the one-loop case [14),17)], and we can see that there is no divergence if $\bar{s} < -\frac{2}{3}$. Moreover, the singularity is found to be a cut because, from our estimates of the period matrix it follows that $(\det A)^2$, that occurs in the denominator of the multiloop integrand, behaves like $(\log \varepsilon)^2$. The treatment given here is essentially the same as the one first given by Lovelace [1)], the only differences being that he worked directly with the open Riemann surface of the analogue model and considered a hole shrinking to zero, and that we have included the measure in our considerations.

If there are no particles attached to the vanishing boundary line it follows that there is no logarithmic factor in the variational formula for $V^*(q_i, q_o; q_j, q_o')$. Therefore, using Eq. (3.8) one readily shows that

$$\exp\left\{-\frac{1}{2}\sum_{i,j} p_i p_j V^*(q_i q_o; q_j q_o')\right\} - \exp\left\{-\frac{1}{2}\sum_{i,j} p_i p_j V(q_i q_o; q_j q_o')\right\} = O(\varepsilon^2) \tag{3.33}$$

and combining this result with the behaviour of the partition function given by Eq. (3.25) we conclude that the integral of the left-hand side of Eq. (3.33) is finite.

The main conclusion of this section is, therefore, the following: if the diagram is non-planar and there is momentum entering into the vanishing boundary line, the integral is

convergent in the parabolic limit of integration. Otherwise it diverges, but the counterterm is given by Eq. (3.33) in terms of the exponential of the Green function of the sphere without the handle that vanishes. The counterterm is, therefore, just the Veneziano integrand for (M-1) loops but integrated, however, with the M loop measure. This simple observation readily explains the duality properties of the counterterm and the fact that double poles rather than single poles occur in some energy variables [20]. One can easily convince oneself that the Neveu-Scherk procedure [20] for regularizing the single-loop amplitude is a particular case of the result described above.

One final word of caution concerning the interpretation of Eq. (3.33): if we want to write an explicit formula for $V(q_i,q_o;q_j,q'_o)$ in terms of Burnside autoromorphic functions [12] in the "vertical" configuration, we have to keep the M generators (one of them being, of course, parabolic). The genus of the surface [18], that is to say, the number of handles, will be (M-1), because of the presence of a parabolic cycle in the boundary of the fundamental region of the group of automorphisms [11]. However, it must be kept in mind that in this case Burnside's proof [12] of convergence does not apply.

iv) Multiple divergencies

The extension of the previous results to the case in which several generators become simultaneously parabolic is straightforward because of the additivity of the results of domain variational theory [5] up to and including terms in ε^2. Therefore, the most singular part of the multiloop integrand in the limit in which two generators, say, T_μ and T_ν become simultaneously parabolic is given by the exponential of the Green function of the sphere with (M-2) handles. It is also simple to construct an integrand which is finite at the end points of the integration region corresponding to T_μ and/or T_ν

becoming parabolic. If we introduce sub-indices μ , ν in V to indicate Green functions of surfaces where the corresponding handles have been eliminated, one can immediately check that the weighted integral of

$$\exp\left\{-\tfrac{1}{2}\sum_{i,j} p_i p_j V(q_i q_o ; q_j q'_o)\right\} - \exp\left\{-\tfrac{1}{2}\sum_{i,j} p_i p_j V_\mu(q_i q_o ; q_j q'_o)\right\} -$$

$$- \exp\left\{-\tfrac{1}{2}\sum_{i,j} p_i p_j V_\nu(q_i q_o ; q_j q'_o)\right\} + \exp\left\{-\tfrac{1}{2}\sum_{i,j} p_i p_j V_{\mu\nu}(q_i q_o ; q_j q'_o)\right\} \tag{3.34}$$

is finite in the limits K_μ and/or $K_\nu \to 1$. In the same way it is possible to write an expression that is finite when N generators become parabolic in all possible ways, but we shall not discuss this point here because the procedure becomes very tedious and it is not all clear at the moment whether it is meaningful from a physical point of view.

It has been shown previously that for the class of diagrams we are considering here there are at most (N+1) parabolic points if the multipliers of the group of automorphism are required to be different from zero. This does not contradict the statement that this class of diagrams shows (2^N-1) parabolic points [16]. Indeed, as discussed before, the extra parabolic points show up only when some generator has multiplier zero and they can be understood as divergencies associated with loops of lower order, because setting a multiplier equal to zero is equivalent to factorizing an internal Reggeon. One can wonder why the multiloop amplitudes we are considering show (N+1) divergencies if there are only N handles. The reason is that divergencies are associated with the number of boundaries rather than with the number of handles. We have seen before that a divergence occurs every time that a handle vanishes in such a way that it forces an internal boundary line to vanish, but the choice of the "external boundary line" is

topologically irrelevant. In case the reader finds it hard to imagine how the external boundary can possibly vanish we have illustrated the example of the two-loop amplitude in Fig. 10, in which all the boundary lines are explicitly shown to be on an equal footing. Two handles and two boundaries can be eliminated, but the choice of the boundary that survives is arbitrary.

It should be clear at this stage that domain variational theory does not provide a natural way of eliminating all $(N+1)$ divergences at once. Indeed, after all N handles have been subtracted there is nothing else than can happen to the surface. This is not a problem at all, because our method is sufficient to give the most singular behaviour of the multiloop integrand in all possible end points of integration. It is only a problem if one insists that it is physically meaningful to keep adding and subtracting ever increasing numbers of counterterms and if one also insists on writing a global counterterm that renders the amplitude finite. Moreover, this problem occurs only for the planar N loop diagram. If the diagram is non-planar, the integral does not diverge in at least two of the parabolic points, and our results are sufficient to construct over-all counterterms that render the amplitude finite. Moreover, it is also clear that some $K_\alpha = 1$ singularities can be simultaneous with $K_\alpha = 0$ singularities. This corresponds, for example, to the extra parabolic points that occur whenever a Reggeon has been previously factorized.

In connection with the planar multiloop amplitude, a regularization procedure has been discussed by Cremmer and Neveu [21] and we would like to interpret their procedure from our point of view. Let us restrict, for simplicity, to the two-loop case. Their procedure consists of introducing first a counter term to cancel the divergence associated with the vanishing of the "external" boundary, that is to say, the boundary where all particles are implanted. Both the initial amplitude and the counter-

term are still divergent when the two other boundaries vanish, so they introduce six other counterterms to take away that divergence.

Cremmer and Neveu find that the momentum dependent part of the counterterm associated with the external boundary is the same as that of the Born approximation [21]. In order to understand this point, we start by investigating what happens when a handle vanishes in such a way that it forces the boundary where all particles are implanted to shrink to zero. In terms of Fig. 9, all particles are now attached to the circle γ_1, but, of course, there is no Pomeranchuk-like singularity because of momentum conservation. Therefore, we find

$$V_M(q_i q_o; q_j q_o') = V_{M-1}(q_i q_o; q_j q_o') + O(\varepsilon^2) \tag{3.35}$$

and all points q_i, q_j lie on the cycle γ_1, that shrinks to zero with the handle. In other words, all pairs of points q_i, q_j tend to coincide in this limit. We now remind the reader that $V_{M-1}(q_i, q_o; q_j, q_o')$ is perfectly regular at the points q_1, q_2 and that the only singularity that could concern us in the limit we are taking is the logarithmic singularity that it exhibits when $q_i \to q_j$

$$V_{M-1}(q_i q_o; q_j q_o') = \log|q_i - q_j| + \text{terms regular when } q_i \to q_j \tag{3.36}$$

The regular part can now be expanded around the point q_1 in the form

$$V_M(q_i q_o; q_j q_o') = \log|q_i - q_j| + A + B_1(q_i - q_1) + B_2(q_j - q_1) + C(q_i - q_1)(q_j - q_1) + \cdots \tag{3.37}$$

The logarithmic term is exactly the Green function of the sphere, $V_o(q_i, q_o; q_j, q_o')$ up to terms that vanish because of momentum conservation. The constant and the linear terms in Eq. (3.37)

are also cancelled because of momentum conservation, and the quadratic terms are of order ε^2. Therefore, we conclude that

$$\exp\left\{-\tfrac{1}{2}\sum_{ij} p_i p_j V_M(q_i q_o; q_j q_o')\right\} - \exp\left\{-\tfrac{1}{2}\sum_{ij} p_i p_j V_o(q_i q_o; q_j q_o')\right\} = O(\varepsilon^2) \tag{3.38}$$

which explains why the counterterm has the same momentum dependence as the Born term, in the particular case in which all particles are attached to the vanishing boundary. The remaining divergences can be taken away from the first term of the left-hand side of Eq. (4.30) in the way discussed before, but there is no natural way of doing the same to the counterterm. Any further regularization has to be done at the expense of changing the partition function part of the measure of integration, which is indeed what Cremmer and Neveu do [21].

The analysis we have given here does not exhaust all multiloop amplitudes. We have essentially covered all diagrams whose group of automorphism contains only hyperbolic generators. The extension of these methods to the case in which there are loxodromic generators is currently under investigation. We would like to stress that their $|K_\alpha| \sim 1$ singularities are a characteristic feature of dual theories. In some particular cases, as the planar one, they appear as a divergence of the amplitude but this is due to the fact that in these cases the singularity is in the square of the sum of all particle momenta which happens to be zero due to momentum conservation.

The specific location of these singularities depends also on the measure of integration and could therefore be shifted in theories whose sewing procedure would provide with different measures. However, their existence is related to the Green function which guarantees the duality of the theory. They seem, therefore, unavoidable. Moreover, they are independent from the loop momentum integration. This fact, which was known for the one-loop case can be recognized in general in the

orientable loop case discussed before from the fact that the first Abelian integral in (A.33) is not singular for $X_\alpha \sim 1$. This contribution was coming from the loop momentum integration or, in other words, the singularity would be the same for every loop momentum.

Therefore, we cannot identify these singularities with some intermediate state. In other words, one uses unitarity to build the theory and one finds that, besides the states that were plugged in, one built up some new ones which have nothing to do with unitarity. The interpretation of these states, characteristic of a dual theory, in the unitarity framework is still far from understood.

ACKNOWLEDGEMENTS

We wish to thank C. Lovelace for enlightening discussions. and D. Olive for useful comments.

A P P E N D I X A

CALCULATION OF THE LOOP INTEGRAND

We shall give here, for the sake of completeness, a slightly refined version of the multiloop calculations carried out in Refs. 1) and 2). The proof is almost identical to the one presented in I, except that zero modes [9] are treated in a somewhat different way. The reader is referred to I for notations and conventions.

In order to derive the multiloop amplitude given by Eq. (2.10) from the N Reggeon vertex given by Eq. (2.3), one has to sew pairs of Reggeons by connecting them with a (twisted or untwisted) propagator, and by taking the trace over oscillator indices and integrating over the loop momenta. The starting point is the matrix elements of the N Reggeon vertex betwcen coherent states.

$$I = \exp\left\{-\frac{1}{2}\sum_{i\neq j}\langle\alpha^i|U^{(i)}V^{(j)}|\alpha^j\rangle\right\} \tag{A.1}$$

We have mentioned in Section 1 how to calculate the matrix elements of a matrix C in terms of the projective transformation associated with it [9]. With respect to the product C_1C_2, either one first multiplies the 2×2 matrices and then applies the rules given by Eqs. (2.7)-(2.8), or one calculates $(C_1C_2)_{nm}$ directly in terms of $(C_1)_{nm}$ and $(C_2)_{nm}$ by the rule [9]

$$(C_1C_2)_{nm} = \sum_{k\neq 0}(C_1)_{nk}(C_2)_{km} + (C_1)_{no}\delta_{0,m} + \delta_{n,0}(C_2)_{om} \tag{A.2}$$

It follows that these infinite matrices from an infinite dimensional representation of the projective group only within the subspace of internal excitations (non-zero modes). We shall rewrite Eq. (A.2) as

$$(C_1 C_2)_{nm} = (C_1 . C_2)_{nm} + (C_1)_{no}\,\delta_{o,m} + \delta_{n,o}\,(C_2)_{om} \tag{A.3}$$

where $(C_1 . C_2)$ means matrix product <u>without zero modes</u> in the intermediate state. Using this notation in Eq. (A.1), together with momentum conservation, we have

$$I = \exp\left\{-\frac{1}{2}\sum_{i\neq j}\langle\alpha^i|U^{(i)}.V^{(j)}|\alpha^j\rangle + \frac{1}{2}\sum_{i=1}^{N} p_i\left[\langle\alpha^i|U^{(i)}|0\rangle + \langle 0|V^{(i)}|\alpha^i\rangle\right]\right\} \tag{A.4}$$

Another important element in the calculation is the fact that, in terms of the symbol Γ introduced in I as the infinite matrix corresponding to the projective transformation

$$\omega = \frac{1}{2} \quad \Rightarrow \quad \tau = \begin{pmatrix} 0 & 1 \\ 1 & 0 \end{pmatrix} \tag{A.5}$$

$$\Gamma = \begin{bmatrix} 0 & 1 & \infty \\ \infty & 1 & 0 \end{bmatrix} \tag{A.6}$$

the following identity is true for infinite matrices

$$A^T = \Gamma A^{-1} \Gamma \tag{A.7}$$

as can be verified by multiplying 2×2 matrices. We warn the reader that Γ, as an infinite matrix, does not exist, and it should never be considered by itself. Equations like (A.7) only make sense if 2×2 matrices are multiplied first and then the matrix elements of the product are computed. Another useful identity is

$$U^{(i)} = V^{(i)T}\Gamma \tag{A.8}$$

valid in any configuration.

a. Trace Calculations

The quadratic term in the coherent state parameters in Eq. (A.4) can be linearized by means of a real functional integral in the space of internal excitations (non-zero modes) as done in Ref. 1) and in I. This step is not at all necessary, but simplifies the presentation of the calculation. Using Eq. (A.8), we get

$$I = [\det\Gamma]^2 \exp\left\{\frac{1}{2}\sum_{i=1}^{N} p_i\left[\langle\alpha^i|U^{(i)}|0\rangle + \langle 0|V^{(i)}|\alpha^i\rangle\right]\right\}$$
$$\int \frac{\delta f}{\sqrt{\pi}} \exp\left\{-\frac{1}{2}\langle f|\Gamma|f\rangle + \sum_{i=1}^{N}\langle f|V^{(i)}|\alpha^i\rangle\right\} \tag{A.9}$$

Let us now put the unsewn Reggeons on the ground state. From now on, we shall denote by N' the number of unsewn Reggeons, and by M the number of pairs of sewn Reggeons with associated Koba-Nielsen variables $z_\mu, \beta_\mu, \tilde{z}_\mu, \tilde{\beta}_\mu$ ($\mu = 1,\ldots,M$), and momenta k_μ and $\tilde{k}_\mu = -k_\mu$, respectively. As in I, we shall keep z_i ($i = 1,\ldots,N'$) as the Koba-Nielsen variables of unsewn Reggeons. By making use of

$$\langle\alpha^i|U^{(i)}|0\rangle = \langle 0|\tilde{U}^{(i)T}|\alpha^i\rangle = \langle 0|\Gamma V^{(i)}|\alpha^i\rangle \tag{A.10}$$

and defining

$$\varphi_i = \langle 0|U^{(i)}|0\rangle + \langle 0|V^{(i)}|0\rangle = \log\left|\frac{z_i(\beta_{i-1}-z_{i+1})}{(z_i-\beta_{i-1})(z_i-z_{i+1})}\right| \tag{A.11}$$

we can rewrite (A.9) as

$$I = (\det\Gamma)^2 \cdot \prod_{i=1}^{N'} e^{\frac{\mu^2}{2}\varphi_i} \cdot \exp\left\{-\frac{1}{2}\sum_{\mu=1}^{M} k_\mu \langle 0|(1+\Gamma)(V_\mu - \tilde{V}_\mu)|\alpha_\mu\rangle\right\} \times$$

$$\times \int \frac{\delta f}{\sqrt{\pi}} \exp\left\{-\frac{1}{2}\langle f|\Gamma|f\rangle + \sum_{i=1}^{N'} p_i \langle z_i|f\rangle + \sum_{\mu=1}^{M} \langle f|\, V_\mu + \tilde{V}_\mu\,|\alpha_\mu\rangle\right\}$$

(A.12)

where $|z_i\rangle = V^{(i)}|0\rangle$ is a vector with components $z_i^n/\sqrt{n}$ $(n \neq 0)$, defined only in the subspace of internal excitations. Using again the identities given by Eqs. (A.8) to write $(\Gamma^2 = I)$

$$\langle 0|(1+\Gamma)\, V_\mu\,|\alpha_\mu\rangle = \langle \alpha_\mu|U_\mu \Gamma(1+\Gamma)|0\rangle = \langle \alpha_\mu|U_\mu(1+\Gamma)|0\rangle$$

and introducing the Hermitian propagator Δ_μ for the μ^{th} Reggeon we have

$$I = [\det\Gamma]^2 \prod_{i=1}^{N'} e^{\frac{\mu^2}{2}\varphi_i} \cdot \exp\left\{-\frac{1}{2}\sum_{\mu=1}^{M}\left[k_\mu \langle \alpha_\mu|\Delta_\mu U_\mu(1+\Gamma)|0\rangle + \right.\right.$$

$$\left.\left. + \tilde{k}_\mu \langle 0|(1+\Gamma)\tilde{V}_\mu|\alpha_\mu\rangle\right]\right\} \times$$

$$\times \int \frac{\delta f}{\sqrt{\pi}} \exp\left\{-\frac{1}{2}\langle f|\Gamma|f\rangle + \sum_{i=1}^{N'} p_i \langle z_i|f\rangle + \sum_{\mu=1}^{M}\left[\langle \alpha_\mu|\Delta_\mu U_\mu \Gamma|f\rangle + \langle f|\tilde{V}_\mu|\alpha_\mu\rangle\right]\right\}$$

(A.13)

From now on, this calculation parallels closely the one presented in I. The next step is to split $|\alpha_\mu\rangle = |\underset{\sim}{\alpha}_\mu\rangle + |\alpha_\mu^0\rangle$ into its zero mode and internal excitation components and to integrate over $|\underset{\sim}{\alpha}_\mu\rangle$. The integrals are of the form

$$\int \frac{1}{\pi}\, \delta \mathrm{Re}\, \underset{\sim}{\alpha}_\mu\, \delta \mathrm{Im}\, \underset{\sim}{\alpha}_\mu\, e^{-\langle \underset{\sim}{\alpha}_\mu|\tilde{\underset{\sim}{\alpha}}_\mu\rangle + \langle \underset{\sim}{\alpha}_\mu|h'_\mu\rangle + \langle h_\mu|\underset{\sim}{\alpha}_\mu\rangle} =$$

$$= e^{-\langle h_\mu|h'_\mu\rangle}$$

(A.14)

but since the integral is in the subspace of internal excitations there are no zero-mode intermediate states in the scalar product $\langle h_\mu | h'_\mu \rangle$ and dots to symbolize their absence must be put in the right places, that is to say, $\langle h_\mu | h'_\mu \rangle = \langle h_\mu | \cdot | h'_\mu \rangle$. We shall not enter here into these straightforward calculations. When the product law (A.3) is used to recombine different terms, the result can be simply written as

$$\mathrm{Tr}\, I = (\det \Gamma)^2 \prod_{i=1}^{N'} e^{\frac{\mu^2}{2}\varphi_i} \exp\left\{ -\sum_{\mu=1}^{M} k_\mu^2 \langle 0 | \frac{(1+\Gamma)}{2} T_\mu \frac{(1+\Gamma)}{2} | 0 \rangle \right\}$$

$$\times \int \frac{\delta f}{\sqrt{\pi}} \exp\left\{ -\frac{1}{2}\langle f | \Gamma | f \rangle + \sum_{\mu=1}^{M} \langle f | T_\mu \Gamma | f \rangle + \sum_{i=1}^{N'} p_i \langle z_i | f \rangle \right\}$$

$$\times \exp\left\{ \sum_{\mu=1}^{M} \frac{k_\mu}{2} \langle 0 | (1+\Gamma)(T_\mu - T_\mu^{-1})\Gamma | f \rangle \right\} \tag{A.15}$$

$$T_\mu = \tilde{V}_\mu \Delta_\mu U_\mu \tag{A.16}$$

Before doing the δf functional integral, let us examine the matrix element $\langle f | T_\mu \Gamma | f \rangle$. Since this is a real symmetric quadratic form in the f_n, we can write

$$\langle f | T_\mu \Gamma | f \rangle = \frac{1}{2}\left\{ \langle f | T_\mu \Gamma | f \rangle + \langle f | (T_\mu \Gamma)^T | f \rangle \right\} \tag{A.17}$$

However, using Eq. (A.7)

$$(T_\mu \Gamma)^T = \Gamma (T_\mu \Gamma)^{-1} \Gamma = \Gamma^2 T_\mu^{-1} \Gamma = T_\mu^{-1} \Gamma \tag{A.18}$$

so that Eq. (A.17) can be written as

$$\langle f | T_\mu \Gamma | f \rangle = \frac{1}{2} \langle f | (T_\mu + T_\mu^{-1}) \Gamma | f \rangle \tag{A.19}$$

Introducing

$$\Sigma = \sum_{\mu=1}^{M} (T_\mu + T_\mu^{-1})$$

we can write

$$-\frac{1}{2} \langle f | \Gamma | f \rangle + \sum_{\mu=1}^{M} \langle f | T_\mu \Gamma | f \rangle = -\frac{1}{2} \langle f | (1-\Sigma) \Gamma | f \rangle \tag{A.20}$$

The δf functional integral can now be made as in I, with the result:

$$Tr\, I = \frac{1}{[\det(1-\Sigma)]^2} \prod_{i=1}^{N'} e^{\frac{\mu^2}{2}\varphi_i} \exp\left\{ -\sum_{\mu=1}^{M} k_\mu^2 \langle 0 | \frac{(1+\Gamma)}{2} T_\mu \frac{(1+\Gamma)}{2} | 0 \rangle \right\}$$

$$\cdot \exp\left\{ -\frac{1}{2} \sum_{i,j} p_i p_j \langle z_i | \Gamma \frac{1}{1-\Sigma} | z_j \rangle - \sum_{i,\mu}{}' p_i k_\mu \bar{\varphi}_\mu(z_i) - \right.$$

$$\left. - \sum_{\nu,j}{}' k_\nu p_j \bar{\varphi}_\nu(z_j) - \frac{1}{2} \sum_{\mu,\nu} k_\mu k_\nu \bar{\varphi}_\mu(z_i) \bar{A}_{\mu\nu} \bar{\varphi}_\nu(z_j) \right\} \tag{A.21}$$

where

$$\bar{\varphi}_\mu(z_i) = \langle z_i | \Gamma \frac{1}{1-\Sigma} \cdot (T_\mu^{-1} - T_\mu) \frac{(1+\Gamma)}{2} | 0 \rangle \tag{A.22}$$

$$\bar{\phi}_\nu(z_j) = \langle 0 | \frac{(1+\Gamma)}{2} (T_\nu - T_\nu^{-1}) \Gamma \cdot \frac{1}{1-\Sigma} | z_j \rangle \tag{A.23}$$

$$\bar{A}_{\mu\nu} = \langle 0 | \frac{(1+\Gamma)}{2} (T_\nu - T_\nu^{-1}) \Gamma \cdot \frac{1}{1-\Sigma} \cdot (T_\mu^{-1} - T_\mu) \frac{(1+\Gamma)}{2} | 0 \rangle \tag{A.24}$$

In Eq. (A.21), the indices i, j run over all the external particles and μ, ν over all the sewn Reggeons. As in I, the operator $(I-\Sigma)^{-1}$ has to be taken with caution. The absence of diagonal terms $i=j$ in the original vertex means that $(1-\Sigma)^{-1}$ has to be taken as the sum of the identity operator plus all the elements of the group G generated by the T_μ, $\mu = 1,\ldots,M$. Moreover, if the index i is equal to j the identity must be omitted in the matrix element $\langle z_i | \Gamma \frac{1}{1-\Sigma} | z_i \rangle$

b. Identification of Abelian Integrals

Let us start by considering the matrix elements

$$\langle z_i | \Gamma \frac{1}{1-\Sigma} | z_j \rangle = \sum_\alpha \langle z_i | \Gamma T_\alpha | z_j \rangle \tag{A.25}$$

where the summation extends over all the elements of the group generated by the T_μ operators. It must be kept in mind that these matrix elements are computed in the subspace of internal excitations. Since $|z_i\rangle = V^{(i)}|0\rangle$ has components $z_i^n/\sqrt{n}$ $(n>0)$; it follows from Eq. (A.8) that

$$\langle z_i | \Gamma = \langle 0 | V^{(i)T} \Gamma = \langle 0 | U^{(i)} \tag{A.26}$$

and, therefore, its components are given by $U^{(i)}_{on} = (z_i^{-n})/(\sqrt{n})$. The operator Γ acts here as a sort of a metric operator that defines a

Möbius invariant Hermitian adjoint. When the Koba-Nielsen variables are on the unit circle this Hermitian adjoint $\langle z_i | \Gamma$ coincides with the usual one because $z^{-1} = z^*$. If we denote by $T_\alpha(z)$ the projective transformation associated with the infinite matrix T_α, the matrix elements (A.25) can be easily computed

$$\langle z_i | \Gamma \frac{1}{1-\Sigma} | z_j \rangle = \sum_\alpha \log \left| 1 - \frac{T_\alpha(z_i)}{z_i} \right| - \sum_\alpha \log \left| 1 - \frac{T_\alpha(0)}{z_i} \right|$$

$$= \sum_\alpha \log |z_i - T_\alpha(z_j)| - \sum_\alpha \log |z_i - T_\alpha(0)|$$

$$= \mathrm{Re}\, \omega_{z_j z_0}(z_i) \tag{A.27}$$

where $\omega_{z_j z_0}(z_i)$ is the third Abelian integral of a sphere with M handles, and Eq. (A.27) corresponds to its representation in terms of a Poincaré Q series of a group of automorphisms [12] with M generators, $T_\mu(z)$. The point z_0 denotes the origin in the complex plane where the automorphic functions are being constructed. When the matrix element given by Eq. (A.27) is multiplied by $p_i p_j$ and summed over all i, j the z_0 dependent term disappears because of momentum conservation.

Let us now focus our attention in the matrix element $\phi_\mu(z)$ defined by Eq. (A.22). We shall denote by $T_\mu(z)$ the projective transformation associated with the generator T_μ. Let us first split $\phi_\mu(z)$ into two parts

$$\bar{\phi}_\mu(z) = \frac{1}{2} \langle z_i | \Gamma \frac{1}{1-\Sigma} \cdot (T_\mu^{-1} - T_\mu) | 0 \rangle + \frac{1}{2} \langle z_i | \Gamma \frac{1}{1-\Sigma} \cdot (T_\mu^{-1} - T_\mu) \Gamma | 0 \rangle \tag{A.28}$$

and examine the first term of the right-hand side. Using Eq. (A.3) and the fact that the sums extend over all the elements of the group of automorphisms, we get:

$$\langle z_i | \Gamma \frac{1}{1-\Sigma} \cdot (T_\mu^{-1} - T_\mu) | 0 \rangle = \sum_\alpha \langle z_i | \Gamma (T_\alpha \circ T_\mu^{-1}) | 0 \rangle - \sum_\alpha \langle z_i | \Gamma (T_\alpha \circ T_\mu) | 0 \rangle$$

$$= \sum_\alpha \langle z_i | \Gamma (T_\alpha T_\mu^{-1}) | 0 \rangle - \sum_\alpha \langle z_i | \Gamma (T_\alpha T_\mu) | 0 \rangle =$$

$$= \sum_{\alpha'} \langle z_i | \Gamma T_{\alpha'} | 0 \rangle - \sum_{\alpha'} \langle z_i | \Gamma T_{\alpha'} | 0 \rangle \equiv 0$$

The same argument cannot be applied to the second term of the right-hand side because $T_\mu^{-1}\Gamma$ and $T_\mu \Gamma$ are not elements of the group. If we denote the 2×2 matrix associated with $T_\mu(z)$ by

$$\tau_\mu = \begin{pmatrix} a_\mu & b_\mu \\ c_\mu & d_\mu \end{pmatrix}$$

it is quite straightforward to compute $(T_\mu \Gamma)_{no}$ and $(T_\mu^{-1}\Gamma)_{no}$ using Eq. (1.3) and get the result

$$(T_\mu \Gamma)_{no} = \frac{1}{\sqrt{n}} \left(\frac{a_\mu}{c_\mu}\right)^n = \frac{1}{\sqrt{n}} J_\mu^{n-1}$$

$$(T_\mu^{-1}\Gamma)_{no} = \frac{1}{\sqrt{n}} \left(-\frac{d_\mu}{c_\mu}\right)^n = \frac{1}{\sqrt{n}} J_\mu^n \qquad \text{(A.29)}$$

where J_μ and J_μ^{-1} are the centres of the isometric circles of $T_\mu(z)$ and $T_\mu^{-1}(z)$, respectively. Then, Eq. (A.28) can be rewritten as

$$\phi_\mu(z) = \frac{1}{2} \sum_\alpha' \langle z | \Gamma T_\alpha | J_\mu \rangle - \frac{1}{2} \sum_\alpha \langle z | \Gamma T_\alpha | J_\mu^{-1} \rangle =$$

$$= \frac{1}{2} \sum_\alpha' \log |z - T_\alpha(J_\mu)| - \frac{1}{2} \sum_\alpha' \log |z - T_\alpha(J_\mu^{-1})|$$

$$= -\pi \, \mathrm{Im}\, \phi_\mu(z) + \pi \, \mathrm{Im}\, \phi_{\mu^{-1}}(z) \qquad \text{(A.30)}$$

where $\phi_\mu(z)$ $(\mu = 1,\ldots,M)$ is one of the first Abelian integrals of a sphere with M handles in the complex normalization, as given by Burnside [12], associated with the μ^{th} handle. It is quite straightforward to show that $\phi_{\mu-1}(z) = -\phi_\mu(z)$ following his normalization proof of first Abelian integrals; so we conclude that the matrix element $\bar{\phi}_\mu(z)$ is directly the imaginary part of the first Abelian integral $\phi_\mu(z)$ in the complex normalization.

Let us now consider the matrix $\bar{A}_{\mu\nu}$ for $\mu \neq \nu$. Using the same arguments as before we can eliminate a term in the right-hand side of the matrix element

$$\sum_\alpha T_\alpha \cdot (T_\mu^{-1} - T_\mu)\left(\frac{1+\Gamma}{2}\right) = \frac{1}{2}\sum_\alpha T_\alpha (T_\mu^{-1} - T_\mu)\Gamma$$

Using

$$\Gamma T_\nu \Gamma = (T_\nu^{-1})^T$$

$$\Gamma T_\nu^{-1} \Gamma = T_\nu^T$$

we can apply the group multiplication law to the left (we need the transposed matrices for this) and eliminate another term. The matrix element simplifies to

$$\bar{A}_{\mu\nu} = \frac{1}{4}\langle 0|(T_\nu - T_\nu^{-1})\Gamma \cdot \frac{1}{1-\Sigma}\cdot(T_\mu^{-1} - T_\mu)\Gamma|0\rangle =$$

$$= \frac{1}{4}\langle J_\nu|\Gamma \cdot \frac{1}{1-\Sigma}\cdot(T_\mu^{-1} - T_\mu)\Gamma|0\rangle - \frac{1}{4}\langle J_{\nu-1}|\Gamma \cdot \frac{1}{1-\Sigma}\cdot(T_\mu^{-1} - T_\mu)\Gamma$$

$$= -\frac{\pi}{2}\,Im\left[\phi_\mu(J_\nu) - \phi_\mu(J_{\nu-1})\right] \qquad (A.31)$$

where J_ν, $J_{\nu-1}$ are the centres of the isometric circles of T_ν and T_ν^{-1}, respectively. Since the centres of the isometric circles are the points homologous to infinity, we can write

$$\bar{A}_{\mu\nu} = -\frac{\pi}{2} \mathrm{Im}\left[\phi_\mu(T_\nu^{-1}(\infty)) - \phi_\mu(\infty) + \phi_\mu(\infty) - \phi_\mu(T_\nu(\infty))\right] =$$

$$= \pi\, \mathrm{Im}\, B_{\mu\nu}$$

(A.32)

so $\bar{A}_{\mu\nu}$ is proportional to the imaginary part of the period matrix of the first Abelian integrals $\phi_\mu(z)$. We have used the fact that

$$B_{\mu\nu} = \phi_\mu(T_\nu(z)) - \phi_\mu(z)$$

is independent of z.

Care must be exercised with the diagonal elements $\bar{A}_{\mu\mu}$, because in this case the Poincaré θ series are not well defined [12]. It can be shown that the extra diagonal term

$$\langle 0 | \frac{(1+\Gamma)}{2} T_\mu \frac{(1+\Gamma)}{2} | 0 \rangle$$

in Eq. (A.21) combines with $\bar{A}_{\mu\mu}$ to give $\mathrm{Im}\, B_{\mu\mu}$. We have, therefore succeeded in correcting the coefficients of the momenta in Eq. (A.21) with Abelian integrals and period matrices of a sphere with M handles.

c. Loop Momentum Integrations

It is quite straightforward now to carry out the loop momentum integrations [1),2)]. This is simply an M×M Gaussian integral, and the result is

$$\int \prod_{\mu=1}^{M} d^4k_\mu\, T_\nu\, I = \frac{1}{[\det(1-\Sigma)]^2} \frac{1}{[\det A]^2} \prod_{i=1}^{N'} e^{\mu^2 \frac{\varphi_i}{2}} \cdot$$

$$e^{-\frac{1}{2} \sum_{i,j=1}^{N}{}' p_i p_j \left\{ \langle z_i | \Gamma \frac{1}{1-\Sigma} | z_j \rangle + \sum_{\mu,\nu=1}^{M} \mathrm{Im}\,\phi_\mu(z_i) (\bar{A}^{-1})_{\mu\nu}\, \mathrm{Im}\,\phi_\nu(z_j) \right\}}$$

(A.33)

where $A = \mathrm{Im}\, B$ and Σ' mean that the identity in the expansion of $(1-\Sigma)^{-1}$ is not included when $i = j$. As shown before, and explained at length in I, the term in brackets is $\mathrm{Re}\,\Omega_{z_i z_o}(z_j)$, the real part of the third Abelian integral of a sphere with M handles in the real normalization. Momentum conservation allows us to add in the exponent any function that depends on only one of the two variables z_i, z_j. Therefore, we can replace the bracket by the Green function of the sphere with M handles, defined by [5]

$$V(z_i, z_o; z_j, z_o') = \mathrm{Re}\,\Omega_{z_i z_o}(z_j) - \mathrm{Re}\,\Omega_{z_i z_o}(z_o') \tag{A.34}$$

If $M = 0$, $V(z_i, z_o; z_j, z_o')$ is just the logarithm of the anharmonic ratio of the four arguments. If the indices i, j are equal, only the regular part of V has to be taken. Moreover, it has already been discussed in I how to obtain the singularity factor (partition functions) from $[\det(1-\Sigma')]^{-2}$. This completes the proof of Eq. (2.10).

A P P E N D I X B

ESTIMATES OF PERIOD MATRICES NEAR A PARABOLIC POINT

Let us consider a group of automorphisms with $M+1$ hyperbolic generators T_μ, and suppose that one of them, say T_{M+1}, becomes parabolic. We are interested in estimating the period matrix $B_{\mu\nu}$ of the first Abelian integrals near the parabolic limit.

In general, one can write a projective transformation in terms of the multiplier K and invariant points ξ, η as [11]

$$T(z) = \frac{(\xi - K\eta)z - \xi\eta(1-K)}{(1-K)z - (\eta - K\xi)} \tag{B.1}$$

and

$$\Delta = ad - bc = K(\xi-\eta)^2 \tag{B.2}$$

Since $T(z)$ is assumed to be hyperbolic, $0 \leq K < 1$. Moreover, the transformations we deal with in multiloop theory leave a circle (the so-called principal circle) invariant. Then, it follows that the invariant points ξ, η lie on the principal circle.

The centres and radii of the isometric circles of T and T^{-1} are given by

$$J = -\frac{d}{c} = \frac{\eta - K\xi}{(1-K)} \quad ; \quad J^{-1} = \frac{\xi - K\eta}{(1-K)} \tag{B.3}$$

$$R = \sqrt{K}\,\frac{|\xi-\eta|}{(1-K)} \tag{B.4}$$

In the parabolic limit, the isometric circles of T and T^{-1} become tangent, and $\xi \to \eta$ and, at the same time, $K \to 1$ in order to keep the centres and the radius finite.

A parabolic transformation is of the form [11]

$$\frac{1}{T(z) - \tilde{\xi}} = \frac{1}{z - \tilde{\xi}} + c \tag{B.5}$$

or

$$T(z) = \frac{(1 + c\tilde{\xi})\, z - c\tilde{\xi}^2}{cz + (1 - c\tilde{\xi})} \tag{B.6}$$

It is easy to see that Eq. (6) is the limit for $\delta \to 0$ of Eq. (B.1) if we make

$$\xi = \eta + \delta = \tilde{\xi} + \delta$$
$$K = 1 - c\delta \tag{B.7}$$

Let us now consider the intersections of the isometric circles with the principal circle in the "near parabolic" limit. This is most easily done if the principal circle is mapped to the real axis in such a way that the centres of the isometric circles and the invariant points are real. The situation in the near parabolic limit is illustrated in Fig. 11. Since the invariant points are always inside the isometric circles, there are two intersections of the isometric circles with the real axis between them. We call those intersections X_A and X_B.

A simple calculation, using Eqs. (B.3) and (B.4), shows that

$$X_B - X_A = \xi - \eta - \frac{2\delta\sqrt{K}}{1+K} = \delta\left[1 - \frac{2\sqrt{K}}{1+K}\right] \tag{B.8}$$

Using

$$\sqrt{k} = 1 - \frac{c\delta}{2} + O(\delta^2)$$

it follows from Eq. (B.8) that

$$x_B - x_A = O(\delta^2) \quad ; \quad \delta \simeq 1 - k \tag{B.9}$$

Equation (B.9) is a crucial observation for the problem we are considering. It means that the isometric circles tend to approach each other faster than the invariant points and its relevance is due to the fact that x_A is the homologous point of x_B under T_{M+1}, so that

$$B_{\mu,M+1} = \phi_\mu(x_B) - \phi_\mu(x_A) \tag{B.10}$$

Let us now consider the first Abelian integral $\phi_{M+1}(z)$ associated with the generator that becomes parabolic, that is to say, the first Abelian integral normalized in such a way that [5]

$$P_\mu(\phi_{M+1}) = \oint_{C_{2\mu-1}} d\phi_{M+1} = \delta_{\mu,M+1} \quad ; \quad \mu = 1, \ldots, M+1 \tag{B.11}$$

Following Burnside [12], we can write $\phi_{M+1}(z)$ in terms of a Poincaré θ series as follows

$$\phi_{M+1}(z) = \frac{1}{2\pi i} \sum_{\alpha} \log\left[\tau_\alpha(z) - J_{M+1}\right] \tag{B.12}$$

up to a constant that does not contribute to the periods. It is convenient now to split the θ series in three parts: the summation over the cyclic subgroup generated by T_{M+1}, the subgroup generated by the remaining generators, and the crossed terms. It is quite straightforward to evaluate the θ series over the cyclic subgroup (this would be a first Abelian integral of a sphere with only one handle). Consequently, Eq. (B.12) can be rewritten as

$$\phi_{M+1}(z) = \frac{1}{2\pi i} \log\left[\frac{z-\xi}{z-\eta}\right] + \tilde{\phi}_{M+1}(z) \tag{B.13}$$

where $\tilde{\phi}_{M+1}(z)$ is the contribution coming from the remaining subgroup and the crossed terms.

First Abelian integrals have logarithmic singularities on the limit points of the group of automorphism. Limit points are accumulation points of centres of isometric circles of elements of the group, and for the case of groups with more than one generator there is a non-denumerable infinite number of them, and in the case of principal circle groups (our case) they lie on the principal circle inside the isometric circles [11]. We shall use here the fact proved in Burnside's paper [12] that the first Abelian integral $\phi_{M+1}(z)$ has an odd number of logarithmic singularities inside the isometric circles I_{M+1}, I_{M+1}^{-1}, and an even number of logarithmic singularities inside the remaining isometric circles I_μ, I_μ^{-1} ($\mu = 1,\ldots,M$). Indeed, this is the reason why $\phi_{M+1}(z)$ has period 1 (-1) when going around the isometric circle I_{M+1} (I_{M+1}^{-1}) and zero otherwise, because Burnside proved that logarithmic singularities cancel by pairs [12]. In Eq. (B.13) we have explicitly exhibited one logarithmic singularity of ϕ_{M+1} inside I_{M+1} and one inside I_{M+1}^{-1}; so we conclude that the remainder $\tilde{\phi}_{M+1}(z)$ has an even number of logarithmic singularities inside I_{M+1} and I_{M+1}^{-1}. Therefore, the cuts of $\tilde{\phi}_{M+1}(z)$ can be taken entirely inside these isometric circles, there is no branch cut $\tilde{\phi}_{M+1}(z)$ crossing from I_{M+1} to I_{M+1}^{-1}.

The remaining isometric circles of the generators of the group are either to the right of I_{M+1}^{-1} or to the left of I_{M+1}. Using the theorem quoted in Section 2c. on the distribution of isometric circles in a group of automorphisms [11], it is easy to convince oneself that there are no other limit points between ξ and η. Therefore, we conclude that $\tilde{\phi}_{M+1}(z)$ is regular in the interval (ξ,η) and can, therefore, be expanded around the points x_A or x_B.

We can now compute the matrix element $B_{M+1,M+1}$, given by

$$B_{M+1,M+1} = \phi_{M+1}[T_{M+1}(z)] - \phi_{M+1}(z)$$

and independent of z. Then

$$B_{M+1,M+1} = \frac{\log K_{M+1}}{2\pi i} + \tilde{\phi}_{M+1}[T_{M+1}(z)] - \tilde{\phi}_{M+1}(z)$$

$$= \frac{\log K_{M+1}}{2\pi i} + \tilde{\phi}_{M+1}(x_B) - \tilde{\phi}_{M+1}(x_A)$$

So, by the mean value theorem:

$$B_{M+1,M+1} = \frac{\log K_{M+1}}{2\pi i} + O[(x_B - x_A)]$$

Therefore, using Eq. (B.9) we conclude that

$$B_{M+1,M+1} = \frac{\log K_{M+1}}{2\pi i} + O(\delta^2) \quad , \delta \sim 1 - K_{M+1} \tag{B.14}$$

for $K_{M+1} \sim 1$. A similar argument, together with the symmetry of matrix $B_{\mu\nu}$, can be used to prove that the remaining matrix elements are of order $(1-K_{M+1})^2$ near the parabolic limit.

REFERENCES

1) C. Lovelace, Phys.Letters 32B, 703 (1970).

2) V. Alessandrini, CERN Preprint TH.1215 (1970), to be published in Nuovo Cimento.

3) M. Kaku and L.P. Yu, Phys.Letters 33B, 166 (1970), and Berkeley Preprints UCRL-20054, UCRL-20055 and UCRL-20104, to be published.

4) H.B. Nielsen, NORDITA Preprint (1969);
D. Fairlie and H.B. Nielsen, Nuclear Phys. B20, 637 (1970).

5) M. Schiffer and D. Spencer, "Functionals of Finite Riemann Surfaces", Princeton (1954).

6) I. Drummond, Nuovo Cimento 67A, 71 (1970);
G. Carbone and S. Scinto, Nuovo Cimento Letters 3, 246 (1970);
J. Kosterlitz and D. Wray, Nuovo Cimento Letters 3, 491 (1970);
D. Collop, Cambridge preprint DAMTP 70/19, to be published;
L.P. Yu, UCRL Preprint 19714, to be published in Phys.Rev.;
M. Ida, H. Matsumoto and S. Yazaki, Tokyo Preprint UT 70-5 (1970).

7) C. Lovelace, Phys.Letters 32B, 495 (1970).

8) D. Olive, Cambridge Preprint DAMTP 70/33, Nuovo Cimento, in press.

9) V. Alessandrini, D. Amati, M. Le Bellac and D. Olive, CERN Preprint TH.1160 (1970), to be published in Physics Reviews.

10) K. Kikkawa, B. Sakita and M.A. Virasoro, Phys.Rev. 184, 1701 (1969).

11) L. Ford - "Automorphic Functions", Chelsea (1951) ;
J. Lehner - "Discontinuous Groups and Automorphic Functions", American Mathematical Society, Providence, Rhode Island (1964).

12) W. Burnside - Proc.London Math.Soc. 23, 49 (1891).

13) M. Kaku and C.B. Thorn - Phys.Rev. 1D, 2860 (1970).

14) D. Gross, A. Neveu, J. Scherk and J. Schwarz - Phys.Rev. 2D, 697 (1970).

15) M. Kaku and J. Scherk - Berkeley Preprint, to be published.

16) M. Kaku and J. Scherk - Berkeley Preprint, to be published.

17) G. Frye and L. Susskind - Phys.Letters 31B, 537 (1970).

18) G. Springer - "Introduction to Riemann Surfaces", Addison Wesley (1957).

19) E.T. Wittaker and G.N. Watson - "Modern Analysis", Cambridge University Press (1952).

20) A. Neveu and J. Scherk - Phys.Rev. 1D, 2355 (1970).

21) E. Cremmer and A. Neveu - Phys.Letters 33B, 356 (1970).

FIGURE CAPTIONS

Figure 1 Points on the Koba-Nielsen unit circle homologous under the generator T_μ. The action of the generator is indicated by an arrowed line. Case (a) is for an untwisted Reggeon, case (b) for a twisted one.

Figure 2 Canonical cycles on a sphere with M handles.

Figure 3 The Koba-Nielsen complex plane for the one-loop orientable diagrams.

Figure 4 The Riemann surface of the one-loop orientable diagrams, with the boundary lines indicated on it.

Figure 5 The Riemann surface of the one-loop non-orientable diagrams with the boundary line indicated on it.

Figure 6 The sphere with two handles and boundary lines corresponding to different two-loop diagrams.
(a) Diagram with three boundary lines.
(b) Diagram with two boundary lines.
(c) Non-orientable diagram with one boundary line.
(d) Orientable diagram with one boundary line.

Figure 7 The Koba-Nielsen complex plane for two-loop diagrams of type (a), (b), (c) - see text - in the case in which all isometric circles are exterior to one another.

Figure 8 The Koba-Nielsen complex plane for two-loop diagrams of type (a), (b), (c) when the isometric circles I_1^{-1} and I_2 overlap.

Figure 9 Attaching a new handle to a sphere with M handles.

Figure 10 Symmetrical representation of the three boundary lines for a two-loop diagram. Only the visible part of the boundary lines has been drawn.

Figure 11 Invariant points and isometric circles near the parabolic limit.

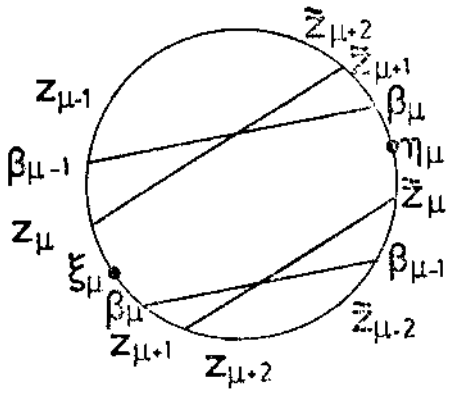

FIG.1a

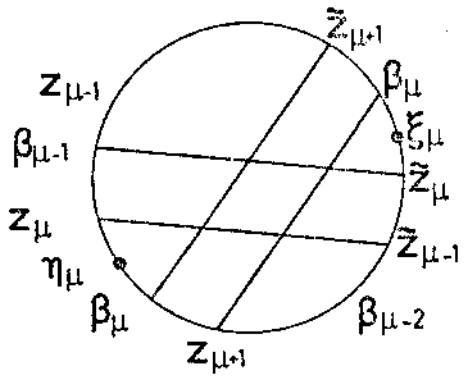

FIG. 1b

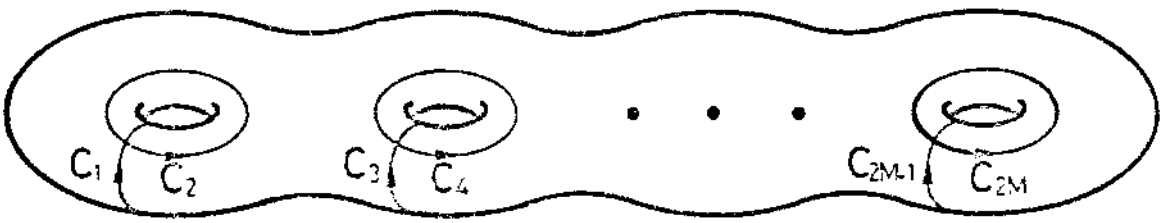

FIG. 2

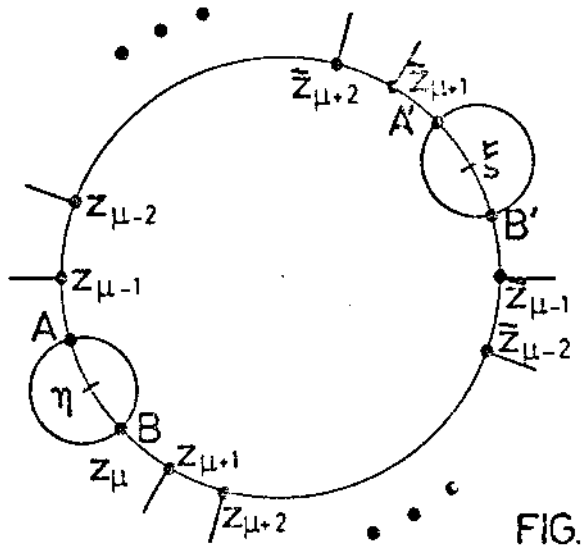

FIG. 3

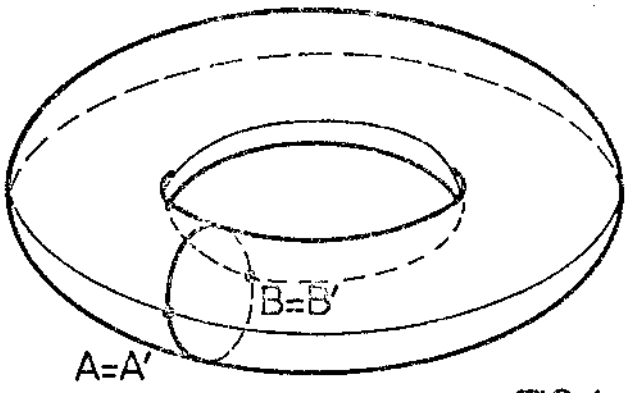

FIG. 4

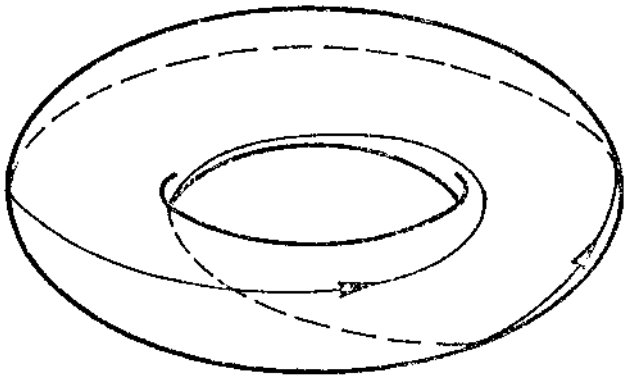

FIG. 5

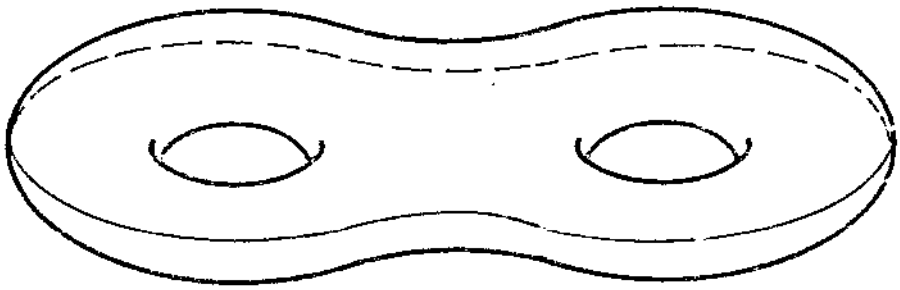

FIG. 6a

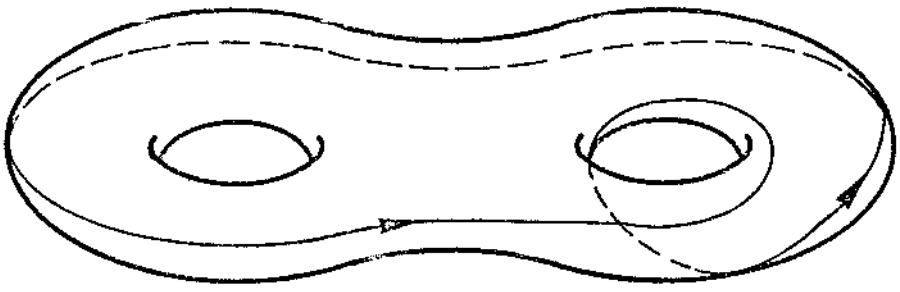

FIG. 6b

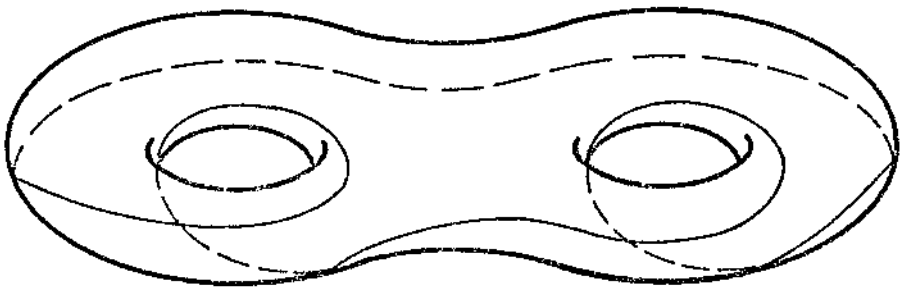

FIG. 6c

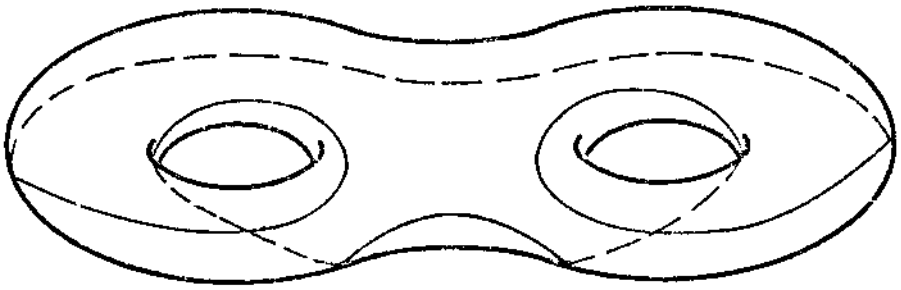

FIG. 6d

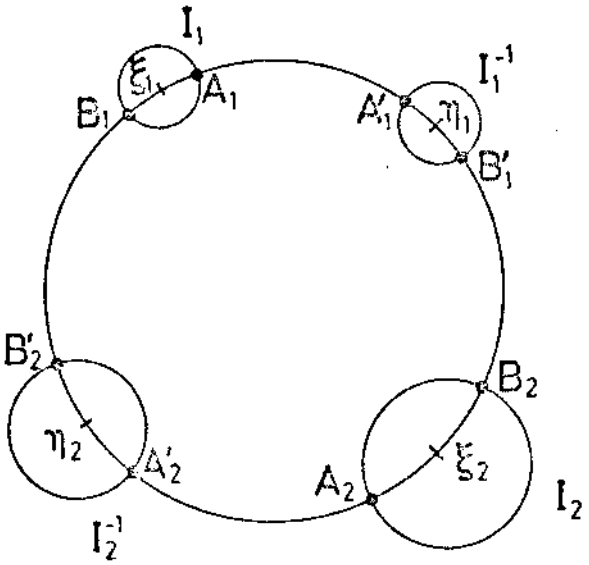
I_1
ξ_1
A_1
B_1
I_1^{-1}
A'_1
η_1
B'_1
B'_2
B_2
η_2
A'_2
A_2
ξ_2
I_2
I_2^{-1}

FIG. 7

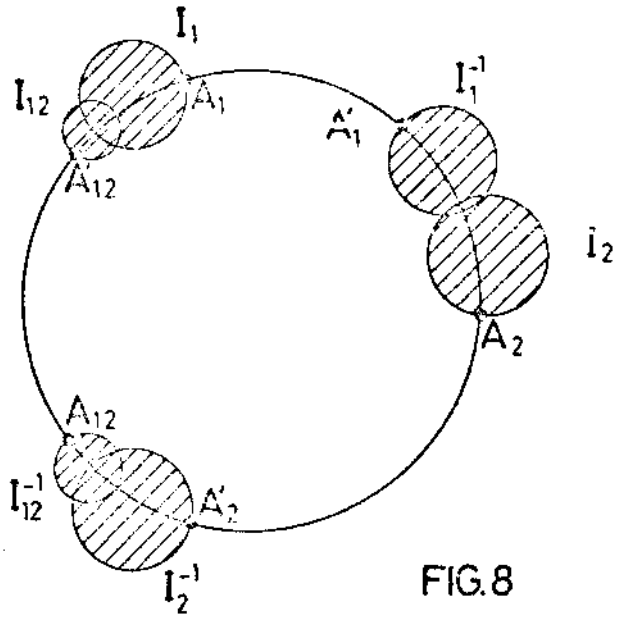
I_1
I_{12}
A_1
I_1^{-1}
A'_1
A_{12}
I_2
A_2
A_{12}
I_{12}^{-1}
A'_2
I_2^{-1}

FIG. 8

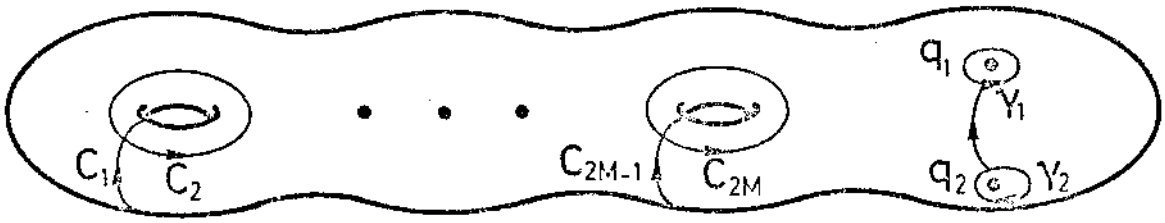

FIG.9

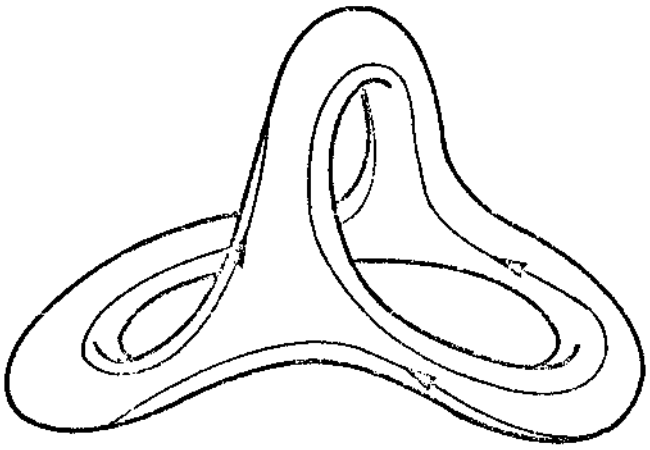

FIG.10

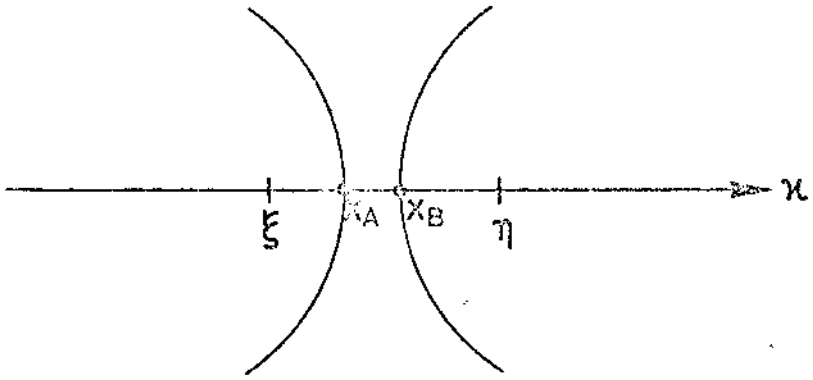

FIG.11